How intramolecular hydrogen bonding (IHB) controls the C-ON bond homolysis in alkoxyamines

Gerard Audran, Raphael Bikanga, Paul Bremond, Mariya Edeleva, Jean-Patrick Joly, Sylvain R.A. Marque, Paulin Nkolo, Valerie Roubaud

Organic & Biomolecular Chemistry

PAPER

View Article Online
View Journal | View Issue

Cite this: *Org. Biomol. Chem.*, 2017, **15**, 8425

How intramolecular hydrogen bonding (IHB) controls the C–ON bond homolysis in alkoxyamines†

Gérard Audran,*[a] Raphael Bikanga,[b] Paul Brémond,[a] Mariya Edeleva,[c] Jean-Patrick Joly,[a] Sylvain R. A. Marque,*[a,c] Paulin Nkolo[a] and Valérie Roubaud[a]

Received 4th September 2017,
Accepted 14th September 2017

DOI: 10.1039/c7ob02223a

rsc.li/obc

Recent amazing results (Nkolo *et al.*, *Org. Biomol. Chem.*, **2017**, 6167) on the effect of solvents and polarity on the C–ON bond homolysis rate constants k_d of alkoxyamine $R_1R_2NOR_3$ led us to re-investigate the antagonistic effect of intramolecular hydrogen-bonding (IHB) on k_d. Here, IHB is investigated both in the nitroxyl fragment R_1R_2NO and in the alkyl fragment R_3, as well as between fragments, that is, the donating group on the alkyl fragment and the accepting group on the nitroxyl fragment, and conversely. It appears that IHB between fragments (*inter* IHB) strikingly decreases the homolysis rate constant k_d, whereas IHB within the fragment (*intra* IHB) moderately increases k_d. For one alkoxyamine, the simultaneous occurrence of IHB within the nitroxyl fragment and between fragments is reported. The protonation effect is weaker in the presence than in the absence of IHB. A moderate solvent effect is also observed.

Introduction

Since the pioneering work of Rizzardo and co-workers,[1,2] alkoxyamines have been applied in several fields such as tin-free radical organic chemistry[3,4] – as initiators for radical cyclization,[5,6] 1,2-radical additions,[7] and several others[5] – NMP (nitroxide mediated polymerization) and its variants: *in situ* NMP,[8] ESCP,[9] NMP2,[10,11] SL-NMP,[12] and CI-NMP,[13] materials sciences – for self-healing polymers,[14] optoelectronic materials,[15] and encoding systems[16] – and in biology,[17–19] as agents for theranostics. For alkoxyamines to be used as agents for theranostics (Fig. 1), the concept of a "smart" alkoxyamine was proposed,[17] that is, a highly stable alkoxyamine switching to a highly labile alkoxyamine through chemical reactions (Fig. 2). For several years, our group has been promoting the chemical alkoxyamine activation using protonation,[20] oxidation,[20] alkylation,[20] or metal cation coordination.[21,22] However, in our view, activation processes based on physicochemical events cannot be disregarded. Indeed, very recently,[23] a dramatic solvent effect on the C–ON bond homolysis rate constant k_d (Scheme 1) has been reported for **1** (Fig. 3). Intramolecular hydrogen-bonding (IHB) displays very different trends, that is, IHB within the nitroxyl fragment affords an

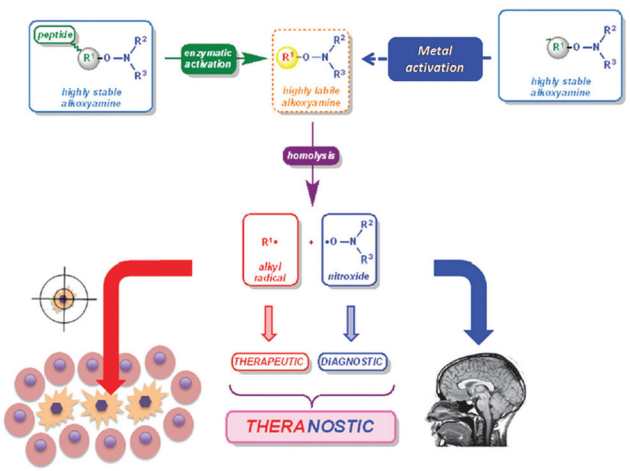

Fig. 1 Concept for the application of alkoxyamines as agents for theranostics. Reproduced with permission of the American Chemical Society (see ref. 46).

[a]*Aix Marseille Univ, CNRS, ICR, UMR 7273, case 551, Avenue Escadrille Normandie-Niemen, 13397 Marseille Cedex 20, France. E-mail: g.audran@univ-amu.fr, sylvain.marque@univ-amu.fr*
[b]*Laboratoire de Substances Naturelles et de Synthèse Organométalliques Université des Sciences et Techniques de Masuku, B.P. 943 Franceville, Gabon*
[c]*N. N. Vorozhtsov Novosibirsk Institute of Organic Chemistry SB RAS, Pr. Lavrentjeva 9, 630090 Novosibirsk, Russia*

† Electronic supplementary information (ESI) available: ^{1}H, ^{13}C NMR and HRMS spectra of **2–7** and **2˙**. DFT calculations for the most stable conformers of **4** and **6**. A gradient profile for flash chromatography. The titration curve for 2-hydroxyethylpyridine, and XRD for *RR*/*SS*-**4** and *RS*/*SR*-**6**. CCDC 1550955 and 1550956. For ESI and crystallographic data in CIF or other electronic format see DOI: 10.1039/c7ob02223a

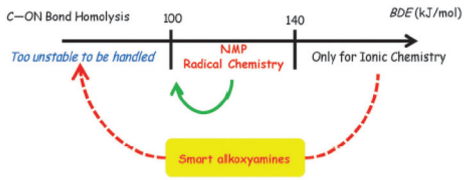

Fig. 2 Concept for "smart" alkoxyamines. Reproduced with permission of the Royal Society of Chemistry (see ref. 17).

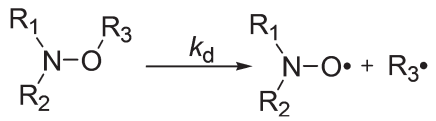

Scheme 1 C–ON bond homolysis in alkoxyamines.

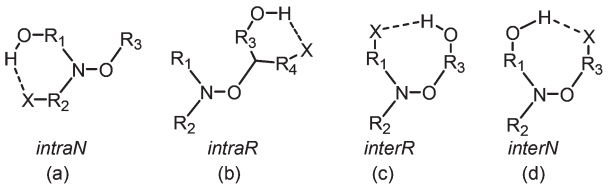

Fig. 4 Various types of IHBs: (a) within the nitroxyl fragment (*intraN*), (b) within the alkyl fragment (*intraR*), (c) from alkyl to nitroxyl fragments (*interR*), and (d) from nitroxyl to alkyl fragments (*interN*). Dotted blue lines represent IHB.

increase in k_d (Fig. 4a)[24–27] and IHB from the alkyl fragment to the nitroxyl fragment (*interR*, Fig. 4c) affords a decrease in k_d spanning from weak (2–3 kJ mol^{-1})[28] to moderate[29] (*ca.* 10 kJ mol^{-1}). Interestingly, other types of IHBs have not yet been investigated – IHB from the nitroxyl fragment to the alkyl fragment (*interN*, Fig. 4d) and IHB within the alkyl fragment (Fig. 4b) – and are the focus of this article. Several models **2–7** (Fig. 3) were prepared and their structures were determined by X-ray and NMR analysis.

The occurrence and the type of IHB were determined by combining ^{31}P and ^{1}H NMR with DFT calculations. The influence of IHB on k_d was investigated in *tert*-butylbenzene (*t*-BuPh) as a non-polar solvent and water as a polar/hydrogen bond acceptor (HBA) solvent, known to suppress IHB.[30]

Results

Preparation of alkoxyamines 2–7

Alkoxyamine **3** was prepared either as previously reported[26] (black route in Scheme 2) or by the hydrolysis[31] of **2** prepared from protected amino alcohol **2a** (blue and magenta routes in Scheme 2). Alkoxyamine **2** was prepared either by the protection[32] of **3** (black route in Scheme 2) or from the protected phosphorylated amino alcohol **2b** (magenta route in Scheme 2).

Alkoxyamine **4** was prepared using the conventional Mn (salen)$_2$ salt procedure (Scheme 3).[33] The two diastereoisomers

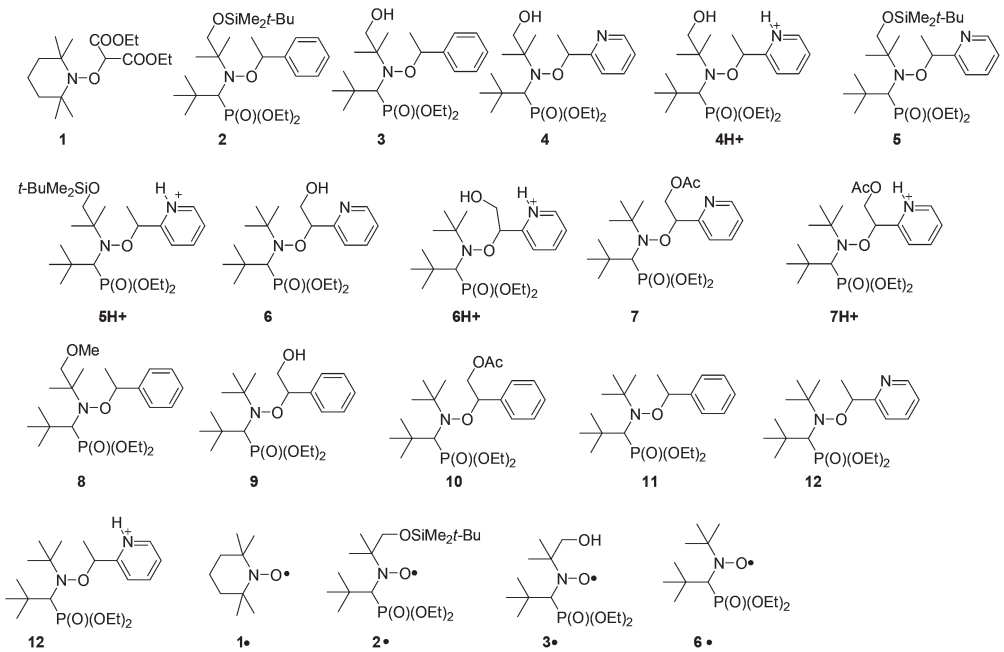

Fig. 3 Alkoxyamines and nitroxides discussed in the article.

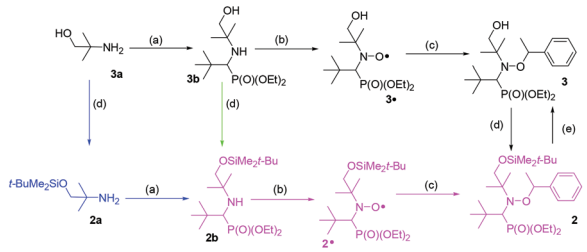

Scheme 2 Preparation of **2** and **3**: (a) (1) **2a** or **3a** (1.1 eq.), *t*-Bu-CHO (1 eq.), pentane, 65 °C, 2 day, (2) $(EtO)_2P(O)H$ (1.1 eq.), 45 °C, 7 days, 64–78%; (b) **2b** or **3b** (1 eq.), Oxone® (4 eq.), Na_2CO_3 (6 eq.), EtOH/H_2O (3 : 1), 5 h, rt, 51–56%; (c) (1) Cu(0) (1.1 eq.), CuBr (0.55 eq.), PMDETA (0.55 eq.), argon bubbled benzene, 30 min, rt, (2) 1-bromoethylbenzene (1.1 eq.), **2**• or **3**• (1 eq.), rt, overnight, 65–72%; (d) **3a**, **3b**, or **3** (1 eq.), *t*-$BuMe_2SiOTf$ (1.5 eq.), 2,6-lutidine (2 eq.), DCM, 4 h, rt 80–90%; (e) **2** (1 eq.) TBAF (1 M in THF) (1.2 eq.), THF, rt, 92%.

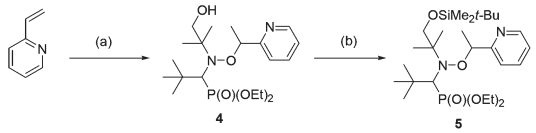

Scheme 3 Preparation of **4** and **5**: (a) (1) salen ligand (0.05 eq.), $MnCl_2$ (0.05 eq.), i-PrOH, 30 min, rt; (2) **3**• (1 eq.), 2-vinyl pyridine (1 eq.), i-PrOH; (3) $NaBH_4$ (5 eq.), 4 h, rt, 54%; (b) (1) **4** (1eq.), pyridine (5 eq.), $AgNO_3$ (1.5 eq.), THF, 5 min, rt; (2) *t*-$BuMe_2SiCl$ (1.5 eq.), overnight, rt, 59–67%.

were separated and *RR*/*SS*-**4** ‡ was recrystallized. Then, it was protected using *t*-$BuMe_2SiCl$ to afford **5** in good yield (Scheme 3).[34] §

Alkoxyamine **6** was prepared from the corresponding bromide **6b** coupled to **6**• using the conventional ATRA procedure.[35] However, **7** was obtained as a crude mixture of diastereoisomers which cannot be separated. Then, crude **7** was hydrolyzed into crude **6** whose diastereoisomers were separated, and the diastereoisomer *RS*/*SR*‡ was crystallized. The diastereoisomers of **6** were acetylated into **7** (Scheme 4).

X-ray analysis

Alkoxyamines *RR*/*SS*-**4** and *RS*/*SR*-**6** were crystallized and analyzed by XRD (Fig. 5).‡ X-ray structures exhibit the conventional distances and angles observed for such types of molecules (see the ESI†). Dihedral angles $<O_5C_6C_7N_8>$ are 45° and 90° larger (Fig. 6d) than the 90° required at TS for *RR*/*SS*-**4** and *RS*/*SR*-**6**, respectively.[36] However, from the X-ray structure (Fig. 5 and 6) it is clear that no IHB occurs in *RR*/*SS*-**4** in the solid state although it is a good model to observe IHB of type (a) or (d) (Fig. 4) or both. By contrast, *RS*/*SR*-**6**, which is a good model for IHB of type (b) or (c) or both (Fig. 4), exhibits only IHB of type (c).¶[37,38] The absence of IHB in the *RR*/*SS*-**4** X-ray

‡ CCDC: 1550955 for *RR*/*SS*-**4** and 1550956 for *RS*/*SR*-**6**.†

§ The procedure described in Scheme 2 was not used because it afforded the isomerization of the pure diastereoisomer.

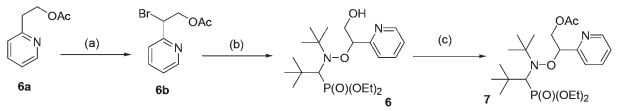

Scheme 4 Preparation of **6** and **7**: (a) **5a** (1 eq.), NBS (1.1 eq.), benzoyl peroxide (0.1 eq.), CCl_4, reflux, 69%; (b) (1) CuBr (0.5 eq.), Cu(0) (1 eq.), PMEDTA (0.5 eq.), benzene, Ar, 10 min, rt; (2) **6**• (1.1 eq.), **6b** (1 eq.), benzene, 12 h, rt, (3) MeOH, K_2CO_3, H_2O, 3 days, rt, 63%; (c) (1) **6** (1 eq.), Et_3N (4 eq.), CH_2Cl_2; (2) Ac_2O (3 eq.), 3 days, rt, 65–90%.

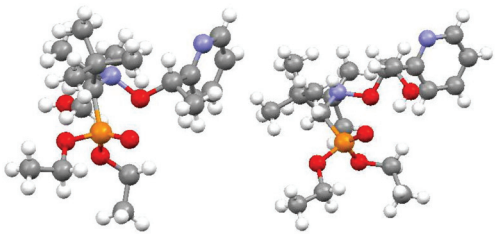

Fig. 5 X-ray structures for *RR*/*SS*-**4** (left) and *RS*/*SR*-**6** (right).‡

structure is in sharp contrast with its occurrence in solution (*vide infra*). This difference in conformation between the crystal and solution has already been observed several times for alkoxyamines[27,28] and it is ascribed to the packing effect, which forces intermolecular H-bonding at the expense of IHB.

NMR analysis

In contrast with XRD, ^1H and ^{31}P NMR spectra show that IHBs of types (a) and (d) occur at the same time for *RR*/*SS*-**4**.‖ As already reported for **2** and **3**,[29] $\Delta\delta$ for **4** and **5** decreases from benzene-d_6 to DMSO-d_6 (Table 1 and Fig. 7), as expected from the increase in the parameter β[30] – the hydrogen bond acceptor (HBA) property of the solvent – that is, the increase in the ability to suppress IHB. The occurrence of IHB between the diethylphosphoryl and the hydroxyl groups (*intraN* in Fig. 8) is supported by the difference in shifts δ and the signal pattern for the $MeCH_2O$ group observed between *RR*/*SS*-**4** and *RR*/*SS*-**5** in benzene-d_6 (protons labelled a in Fig. 9)** and its suppression in DMSO-d_6 (very similar patterns for protons labelled a–c for *RR*/*SS*-**4** and *RR*/*SS*-**5** in Fig. 9). However, the chemical shifts δ and the signal pattern of pyridyl protons (Fig. 9) are very different for *RR*/*SS*-**4** and *RR*/*SS*-**5** in benzene-d_6, while they are similar in DMSO-d_6. As similar observations were also reported upon protonation (or other types of activation) of the pyridyl moiety in alkoxyamines,[20–22] this change in the signal is ascribed to the occurrence of IHB between the hydroxyl group and the pyridyl moiety (*interN* in Fig. 8). Temperature

¶ $d_{P=O\cdots HO}$ = 1.96 Å and $<O_1H_{15}O_{14}>$ = 164°. The bond radii of H, N and O are r_H = 1.09 Å, r_N = 1.55 Å and r_O = 1.52 Å, respectively. See ref. 37.

‖ *RR*/*SS*-**5** exhibiting no IHB was chosen as a model for **4** and very similar solvent effects were expected.

** Protons from CH_2OH (labelled e in Fig. 9) are expected to be sensitive to the silylation of the hydroxyl functions, whereas protons labelled b and c are not expected to be very sensitive.

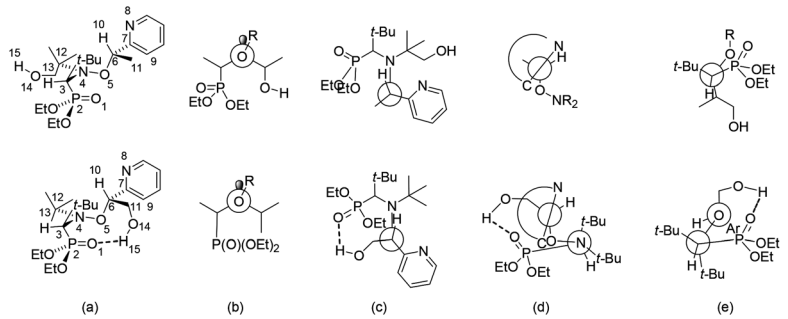

Fig. 6 Cram (a) and Newman projections through (b) N_4–O_5, (c) O_5–C_6, (d) C_6–C_7, and (e) C_3–N_4 bonds for *RR*/*SS*-**4** (top) and *RS*/*SR*-**6** (bottom).

Table 1 Solvent effect on diastereoisomers of **4** and **5** investigated by ^{31}P NMR

		δ (ppm)			δ (ppm)		
Solvent[a]	β[b]	*RR*/*SS*-**4** [c]	*RR*/*SS*-**5** [c]	$\Delta\delta$[d] (ppm)	*RS*/*SR*-**4** [c]	*RS*/*SR*-**5** [c]	$\Delta\delta$[d] (ppm)
$CDCl_3$	0.10	27.29	26.11	1.18	26.13	25.22	0.91
C_6D_6	0.10	27.35	25.86	1.49	26.29	24.95	1.34
CD_3CN	0.40	27.17	26.25	0.92	26.57	25.25	1.32
Acetone-d_6	0.48	27.27	26.31	0.96	26.69	25.21	1.48
CD_3OD	0.66	27.32	27.04	0.28	26.42	26.02	0.40
DMSO-d_6	0.76	26.46	26.15	0.31	25.61	24.95	0.66

[a] 85% H_3PO_4 was used as an internal reference (0 ppm). [b] Hydrogen bond acceptor parameter β. Given in ref. 30. [c] Ratio **4** : **5** = 2 : 1. [d] $\Delta\delta = \delta_4 - \delta_5$.

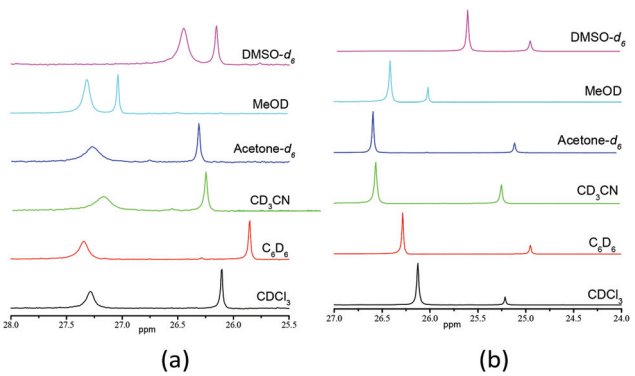

Fig. 7 ^{31}P NMR signals in various solvents for (a) a (2 : 1) mixture of *RR*/*SS*-**4** (left) and *RR*/*SS*-**5** (right), and (b) a (2 : 1) mixture of *RS*/*SR*-**4** (left) and *RS*/*SR*-**5** (right).

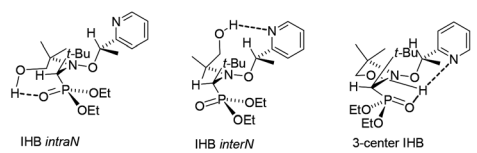

Fig. 8 Possible conformations affording *intraN* IHB (left), *interN* IHB (middle), and 3-center IHB (right) for *RR*/*SS*-**4**.

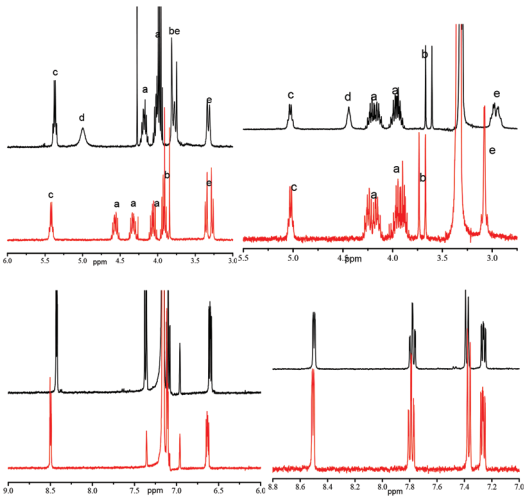

Fig. 9 ^{1}H NMR spectra of *RR*/*SS*-**4** (top) and *RR*/*SS*-**5** (bottom) in the range 2.5–6 ppm (top row) and 6–9 ppm (pyridyl proton zone, bottom row) in benzene-d_6 (left) and DMSO-d_6 (right). Labelling of protons: a–e represent MeCH_2O, *CH*P, *CH*Me, *OH*, and CH_2O, respectively.

dependence shows only line broadening when the temperature is decreased down to −80 °C, meaning that the rotation around the C–N bond of the group carrying the hydroxyl function is faster than the resolution time of ^{1}H NMR. DFT calculations (*vide infra*) led us to disregard the occurrence of 3-center IHB, as shown in Fig. 8.

The same trends are observed for $\Delta\delta$ (Fig. 7 and Table 1) and ^{1}H NMR signals of EtO protons (labelled a in Fig. 1SI†) for *RS*/*SR* diastereoisomers of **4** and **5** as those for diastereoisomers *RR*/*SS* and are ascribed to the occurrence of IHB between the diethylphosphoryl and the hydroxyl groups (Fig. 10). In sharp contrast to what was observed for the diastereoisomer *RR*/*SS*, no significant differences in chemical shifts and signal patterns in the pyridyl proton zone are observed for *RS*/*SR*-**4** and *RS*/*SR*-**5**, whatever the solvent (Fig. 1SI†). Consequently, only *intraN* IHB (type (a) in Fig. 4) is observed in *RS*/*SR*-**4** (Fig. 10a).

The same trends are observed for $\Delta\delta$ (Fig. 11b and Table 2) and ^{1}H NMR signals of EtO protons (labelled a in Fig. 2SI†) for *RS*/*SR* diastereoisomers of **6** and **7** as those for **4** and **5** (*vide*

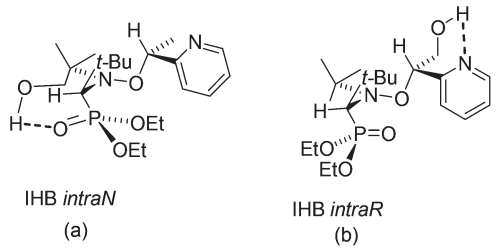

Fig. 10 Possible conformations affording *intraN* IHB for *RS*/*SR*-**4** (a) and *intraR* IHB for *RR*/*SS*-**6** (b).

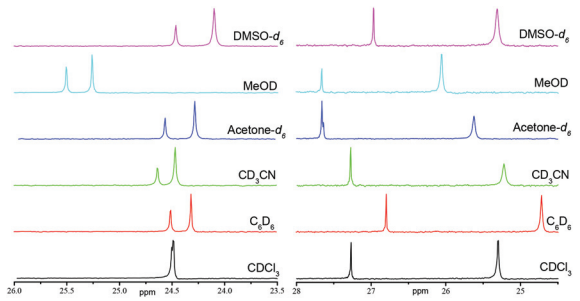

Fig. 11 ^{31}P NMR signals in various solvents for (a) a (2 : 1) mixture of *RR*/*SS*-**6** (left) and *RR*/*SS*-**7** (right), and (b) a (2 : 1) mixture of *RS*/*SR*-**6** (left) and *RS*/*SR*-**7** (right).

Table 2 Solvent effect on diastereoisomers of **6** and **7** investigated by ^{31}P NMR

		δ (ppm)			δ (ppm)		
Solvent[a]	β[b]	*RR*/*SS*-**6**[c]	*RR*/*SS*-**7**[c]	$\Delta\delta$[d] (ppm)	*RS*/*SR*-**6**[c]	*RS*/*SR*-**7**[c]	$\Delta\delta$[d] (ppm)
$CDCl_3$	0.10	24.48	24.48	0.0	27.27	25.30	1.97
C_6D_6	0.10	24.52	24.32	0.20	26.90	24.82	2.08
CD_3CN	0.40	24.64	24.47	0.17	27.25	25.19	2.06
Acetone-d_6	0.48	24.63	24.34	0.29	27.65	25.62	2.03
CD_3OD	0.66	25.51	25.27	0.24	27.65	26.05	1.60
DMSO-d_6	0.76	24.45	24.08	0.37	26.97	25.30	1.67

[a] 85% H_3PO_4 was used as an internal reference (0 ppm). [b] Hydrogen bond acceptor parameter β. Given in ref. 30. [c] Ratio **6** : **7** = 2 : 1. [d] $\Delta\delta = \delta_6 - \delta_7$.

supra) and are ascribed to the occurrence of IHB between the diethylphosphoryl and the hydroxyl groups (Fig. 6) in *RS*/*SR*-**6**. On the other hand, the very similar signal patterns of protons in the aromatic zone for *RS*/*SR*-**6** and *RS*/*SR*-**7** (Fig. 2SI†) support the non-occurrence of *intraR* IHB (type b in Fig. 4 and 6).

No significant changes in $\Delta\delta$ (Table 2 and Fig. 11b) and in the signal patterns of EtO-groups (protons labelled a in Fig. 3SI†) are observed for *RR*/*SS*-**6** and *RR*/*SS*-**7**, pointing to the absence of *interR* IHB (type c in Fig. 4). By contrast, significant

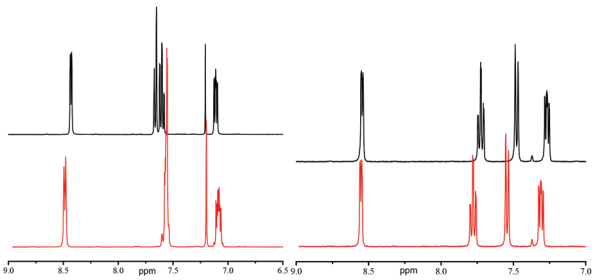

Fig. 12 ^{1}H NMR spectra of *RR*/*SS*-**6** (top) and *RR*/*SS*-**7** (bottom) in the range 3–6 ppm (top row) and 6–9 ppm (pyridyl proton zone, bottom row) in $CDCl_3$ (left) and DMSO-d_6 (right). Labelling of protons: a–e represent MeCH_2O, CHP, CHMe, OH, and CH_2O, respectively.

changes in the signal patterns of aromatics are observed between *RR*/*SS*-**6** and *RR*/*SS*-**7** in benzene-d_6, whereas very similar signal patterns for *RS*/*SR*-**6** and *RS*/*SR*-**7** are observed (Fig. 12) in DMSO-d_6, *i.e.*, the absence of any type of IHB, supporting the occurrence of *intraR* IHB in *RR*/*SS*-**6** in benzene-d_6 (Fig. 10b).

Protonation of alkoxyamines

Alkoxyamines **4**–**7** carry a pyridyl moiety on the alkyl fragment suitable for activation by protonation. Consequently, protonation in benzene-d_6 (model for *tert*-butylbenzene *t*-BuPh) in the presence of trifluoroacetic acid is confirmed by changes in ^{1}H NMR shifts in the aromatic zone, *e.g.* *RR*/*SS*-**4** (Fig. 4SI†). The values of pK_a (Table 3)[39] are estimated from the ^{1}H NMR shift of the signal in the aromatic zone, *e.g.*, *RR*/*SS*-**4** (Fig. 13), and are given by the modified Hasselbach–Henderson equation (eqn (1), exemplified by **4**/**4H+**, and Table 3).[40,41]

$$\delta_{pH} = \delta_{\mathbf{4}} + \frac{\delta_{\mathbf{4H+}} - \delta_{\mathbf{4}}}{1 + 10^{pK_a - pH}} \quad (1)$$

As already reported, the pK_a of **12** is *ca.* 1.7–1.9 units lower than that reported for the *ortho*-ethylpyridine. It is ascribed to the presence of the nitroxyl fragment as a strong electron withdrawing group (EWG). The one unit lower pK_a for the *ortho*-hydroxyethylpyridine is also ascribed to the presence of the OH group as an EWG. Therefore, the lower pK_a values for **4**–**7** (Fig. 13) than those for *ortho*-ethylpyridine and *ortho*-hydroxyethylpyridine are due to the presence of the nitroxyl fragment as an EWG. It is noteworthy that alkoxyamines **4**–**6** exhibit pK_a values very close to those for model **12**, except for *RR*/*SS*-**6**.

The one unit lower pK_a value for **7** than that for **12** is ascribed to the acylated hydroxyl group, which exhibits a higher electron withdrawing property than the OH group, the basicity of the pyridine moiety being thus decreased.

Kinetic investigations

Homolysis rate constants $k_{d,T}$ were measured using either the ^{31}P NMR method[27] for **4**, **4H+**, **5**, **7** and **7H+** or the EPR method[20] for **2**, **2′**, **2″**, **3′**, **6** and **6H+**, as previously reported. Differences in E_a observed between diastereoisomers for **2**, **2′**, **2″**, **3**, **5** and **7** in *t*-BuPh as a solvent are in the range of

Table 3 Values of pK_a for **4–7**

	4		**5**		**6**		**7**	
	RR/*SS*	*RS*/*SR*	*RR*/*SS*	*RS*/*SR*	*RR*/*SS*	*RS*/*SR*	*RR*/*SS*	*RS*/*SR*
pK_a [a,b]	4.08[c]	4.32[c]	3.81[c]	4.25[c]	4.25[c,d]	3.61[c,d]	3.24[c,d]	3.33[c,d]

[a] All pH values measured in D_2O/MeOH-d_4 (1 : 1) were re-estimated using pH = 0.929·pH* + 0.42. pH* is the pH measured in D_2O/MeOH-d_4 solutions using a pH-meter calibrated with non-deuterated water. See ref. 39. [b] pK_a = 5.89 for *ortho*-ethylpyridine. See ref 40. [c] pK_a = 4.85 for *ortho*-2-hydroxyethylpyridine. See the ESI. [d] pK_a values of 4.21 (*RS*/*SR*) and 3.99 (*RR*/*SS*) were reported for **12**. See ref. 41.

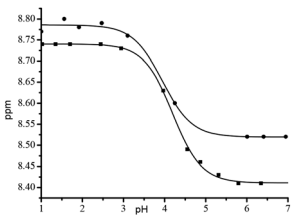

Fig. 13 Titration curves for *RR*/*SS*-**4** (0.01 M, ■, inset: signal of the aromatic proton zone) and *RS*/*SR*-**4** (0.01 M, ●), D_2O/MeOH-d_4 = 1 : 1.

0–2 kJ mol^{-1} – generally observed for diastereoisomers reported in the literature – and do not deserve more comments.[36] Alkoxyamines exhibiting IHB are discussed later. Except for **6**, comments made for diastereoisomers in *t*-BuPh as a solvent hold in water, as IHB is suppressed.

DFT calculations

DFT calculations at the M062X/6-31+G(d,p) level of theory in the gas phase were performed to determine both the thermodynamics of the homolysis and the most stable conformations for the diastereoisomers of **2–4** and **6** (Table 1SI†).[42] Important geometrical parameters – bond lengths, distances and angles – are reported in Table 1SI† and agree with X-ray data and those reported for molecules of the same family, except for the occurrence of IHB in *RR*/*SS*-**4**. Thermodynamics of **4** and **6** show the same trends as that experimentally reported (Table 1SI†). Only the 3 most stable conformations **A**, **B** and **C** †† are reported for **4** and **6** (Fig. 14). Valence angles, bond lengths and distances for IHB are reported in Table 5. Depending both on the valence angle α and on the distance $d_{H\cdots X}$ between the H and X atoms implied in the H-bonding, IHB is given as strong ($\alpha > 150°$ and d smaller than the sum of van der Waals radii of H and X atoms), as weak ($\alpha < 120°$ and d closer to the sum of the van der Waals radii of H and X atoms) or as medium for other combinations.¶[37,38] On these grounds, IHB for the most stable conformers is considered as strong for *RS*/*SR*-**6** (conformer **A**) and *RS*/*SR*-**9**, and as medium for other diastereoisomers (Fig. 14 and Table 5). For all cases, IHB is smaller by *ca*. 1.8 Å and by 0.5 Å for OH···O=P and for OH···N interactions, respectively, than the respective sums of van der Waals radii¶ – $d_{OH\cdots OP}$ = 2.61 Å and $d_{OH\cdots N}$ = 2.64 Å – and all valence angles α are larger than 130°. Nevertheless, the occurrence of IHB is controlled mainly by the steric hindrance. As illustrated by *RR*/*SS*-**9**, when steric hindrance is too large, IHB does not occur, and in some cases, for example, *RR*/*SS*-**4** and *RR*/*SS*-**6**, the most stable conformer **B** does not display the strongest IHB.‡‡ All other possible IHBs are disregarded due to distances $d_{OH\cdots OP}$ and $d_{OH\cdots N}$ much larger than the sums of the van der Waals radii, except for OH···NO for the conformer **C** of *RS*/*SR*-**6**. Nonetheless, the IHB observed between the hydroxyl group and the N atom of the nitroxyl moiety in the conformer **C** is not strong enough to balance the steric strain in **C**, which is less stable than **A** by 19 kJ mol^{-1} (Fig. 14).

Discussion

Free motions in the nitroxyl fragment

Taking into account (i) NMR observations for *RR*/*SS*-**4** denoting the simultaneous occurrence of *intraN* and *interN* IHBs (Fig. 4), (ii) calculations ascribing these two IHBs to two different conformers (Fig. 14 and Table 5), (iii) dramatically restricted bond rotations in the group carrying the diethylphosphoryl group attached to the nitroxyl moiety in nitroxides, and in the subsequent alkoxyamines,§§[43–45] the question of the free rotation around the C–N bond for the other alkyl group attached to the nitroxyl moiety is raised. Indeed, the conformations of the nitroxyl fragment are expected to be ruled by the conformations of the nitroxide, as highlighted by the occurrence of the same IHB in **3**$^{\bullet}$[26] and **3**.[27] Whatever the route for the preparation of **2** and **3** (Scheme 2 and ESI†), ^{1}H NMR spectra of intermediates are the same (see the ESI†) as well as k_d values within the experimental error (Table 4), supporting that for the group carrying the hydroxyl function, the rotation of the C–N bond is free, whereas the rotation of the C–N bond for the moiety carrying the diethylphosphoryl group

†† Conformer **A** exhibiting IHB between HO and P=O functions, conformer **B** exhibiting IHB between the OH function and N atom, and **C** the most stable conformer with no IHB.

‡‡ Indeed, conformer **A** exhibits geometrical parameters (Table 5) featuring stronger IHB than in **B** as highlighted by the shorter $d_{OH\cdots OP}$ and flatter angle α for *RR*/*SS*-**6**.

§§ When the *t*-Bu group attached to the nitroxyl moiety is replaced by a bulkier group CMe_2R, no difference in k_d is observed, meaning that the nitroxyl fragment adopts a conformation which forces the R group to be in such a position that its bulkiness is cancelled. This is due to the levelled steric effect. See ref. 43–46.

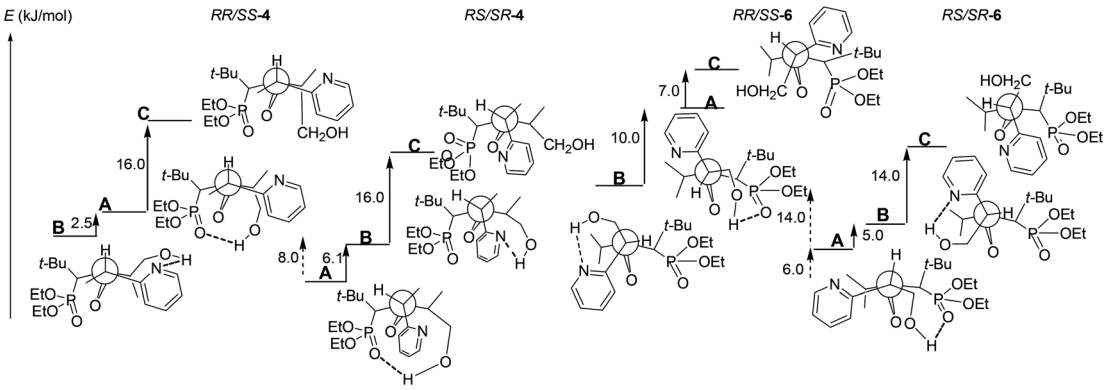

Fig. 14 Most stable conformations **A**–**C**†† for *RR*/*SS*-**4**, *RS*/*SR*-**4**, *RR*/*SS*-**6**, and *RS*/*SR*-**6**. All conformers are on the same energetic scale (kJ mol^{-1}). Dotted lines for the difference in energy between isomers and full lines for the difference in energy between conformers.

Table 4 C–ON bond homolysis rate constant $k_{d,T}$ at various temperatures T for alkoxyamines under various conditions of solvents and pH and their corresponding activation energies E_a, the homolysis rate constant k_d re-estimated at 120 °C and predicted activation energies E'_a

			RR/*SS*			*RS*/*SR*			E'_a [a,b]		
	Solvent	T (°C)	$k_{d,T}$ [c,d]	E_a [b,e]	k_d [f,g]	$k_{d,T}$ [c,d]	E_a [b,h]	k_d [f,i]	*RR*/*SS*	*RS*/*SR*	References[j]
2 [k,l]	*t*-BuPh	90	3.0	124.4	7.1	3.5	123.9	8.2	—[m]	—[m]	t.w.
2′ [l,n]	*t*-BuPh	100	9.4	124.3	7.3	10.5	124.0	8.0	n.d.	n.d.	t.w.
2″ [l,o]	*t*-BuPh	90	3.2	124.2	7.6	3.5	124.0	8.0	n.d.	n.d.	t.w.
3 [l]	*t*-BuPh	n.m.	n.m.	122.5	12.5	n.m.	121.8	15.5	—[p]	—[p]	29
3′ [l,n]	*t*-BuPh	100	14.7	122.9	11.2	16.7	122.5	12.7	n.d.	n.d.	t.w.
4 [q]	*t*-BuPh	80	4.1	120.1	26.1	2.4	121.7	16.0	122.5[r]	122.8[r]	t.w.
4H+ [q]	*t*-BuPh[s]	50	0.8	114.3	154.1	0.6	115.3	113.5	112.2[t]	113.8[t]	t.w.
5 [q]	*t*-BuPh	100	110.0	123.7	8.7	220.0	121.7	16.0	124.4[u]	124.9[u]	t.w.
5H+ [q]	*t*-BuPh	50	1.3	113.1	225.4	1.0	113.7	187.6	115.8[t]	113.8[t]	t.w.
6 [l]	*t*-BuPh	100	23.7	121.5	17.0	2.9	128.0	2.3	123.4[v]	128.9[v]	t.w.
6H+ [l]	*t*-BuPh[s]	83	11.8	117.9	51.2	1.2	124.8	6.2	113.6[t]	120.1[t]	t.w.
7 [q]	*t*-BuPh	83	2.8	122.2	13.7	4.4	120.9	20.4	123.0[w]	124.9[w]	t.w.
7H+ [q]	*t*-BuPh[s]	61	0.5	119.2	34.9	0.8	118.3	45.9	114.1[t]	117.0[t]	t.w.
8	*t*-BuPh	n.m.	n.m.	123.2	10.1	n.m.	122.7	11.8	n.d.	n.d.	27
9	*t*-BuPh	n.m.	n.m.	123.4	9.5	n.m.	129.9	1.3	—[x]	—[x]	29
10	*t*-BuPh	n.m.	n.m.	123.0	10.7	n.m.	123.9	8.1	—[y]	—[y]	29
11	*t*-BuPh	n.m.	n.m.	124.0	7.9	n.m.	123.0	10.7	—[z]	—[z]	29
12	*t*-BuPh	n.m.	n.m.	124.1	7.8	n.m.	123.8	8.4	—[aa]	—[aa]	41
12H+	*t*-BuPh	n.m.	n.m.	116.0		n.m.	116.2		n.d.	n.d.	41
3	—[ab]	n.m.	n.m.	125.1	5.7	n.m.	122.8	11.4	—[ac]	—[ac]	27
4 [q]	pH = 7.0[ad]	80	8.3	118.0	49.6	12.8	116.8	71.7	121.3[ae]	123.6[ae]	t.w.
4H+ [q]	pH = 1.4[ad]	50	4.6	109.6	649.3	4.9	109.4	690.3	104.5[af]	103.3[af]	t.w.
6 [l]	pH = 7.0[ad]	93	14.9	120.3	24.6	5.0	124.1	7.7	118.4[ag]	124.8[ag]	t.w.
6H+ [l]	pH = 1.4[ad]	72	14.6	113.8	179.6	12.8	114.2	158.9	106.8[af]	110.6[af]	t.w.
8	—[ab]	n.m.	n.m.	123.8	8.4	n.m.	123.2	10.1	n.d.	n.d.	29
9	—[ab]	n.m.	n.m.	122.2	13.7	n.m.	124.4	7.0	—[ah]	—[ah]	29
11	—[ab]	n.m.	n.m.	123.0	10.7	n.m.	124.0	7.9	—[z]	—[z]	29
12	—[ab]	n.m.	n.m.	121.4	17.5	n.m.	122.5	12.5	—[ai]	—[ai]	41
12H+	—[ab]	n.m.	n.m.	108.0		n.m.	109.0		n.d.	n.d.	41

[a] Predicted values of E_a using the incremental scale. [b] In kJ mol^{-1}. [c] In 10^{-4} s^{-1}. [d] Given by eqn (4). [e] Estimated using k_d values in the 4th column and the frequency factor $A = 2.4 \times 10^{14}$ s^{-1} in eqn (5). See ref. 51. [f] In 10^{-3} s^{-1}. [g] Estimated using E_a values in the 5th column and the frequency factor $A = 2.4 \times 10^{14}$ s^{-1} in eqn (5). See ref. 51. [h] Estimated using k_d values in the 7th column and the frequency factor $A = 2.4 \times 10^{14}$ s^{-1} in eqn (5). See ref. 51. [i] Estimated using E_a values in the 8th column and the frequency factor $A = 2.4 \times 10^{14}$ s^{-1} in eqn (5). See ref. 51. [j] t.w.: this work. n.d.: not determined. n.m.: not measured. [k] Prepared *via* the route **3a** → **3b** → **3**$^{\bullet}$ → **3** → **2**. [l] Measured by EPR. [m] Used as a model: $\Delta_{11\to2}$ = +0.4 kJ mol^{-1} for the diastereoisomer *RR*/*SS* and $\Delta_{11\to2}$ = +0.9 for the diastereoisomer *RS*/*SR*. [n] Prepared *via* the route **3a** → **2a** → **2b** → **2**$^{\bullet}$ → **2′**(**2**) → **3′** (**3**). [o] Prepared *via* route **3a** → **3b** → **2b** → **2**$^{\bullet}$ → **2″** (**2**). [p] Used as a model: $\Delta_{11\to3}$ = −1.5 for *RR*/*SS* and $\Delta_{11\to3}$ = −1.2 for *RS*/*SR*. [q] k_d determined by ^{31}P NMR. See ref. 20. [r] $E'_a = E_{a,11} + \Delta_{11\to3} + \Delta_{11\to12}$. [s] Protonation is performed by adding 2 eq. of TFA. [t] Protonation expected to decrease E_a by 7.9 kJ mol^{-1}, as highlighted by the protonation of **12** in *t*-BuPh. See ref. 41. [u] $E'_a = E_{a,11} + \Delta_{11\to2} + \Delta_{11\to12}$. [v] $E'_a = E_{a,11} + \Delta_{11\to9} + \Delta_{11\to12}$. [w] $E'_a = E_{a,11} + \Delta_{11\to10} + \Delta_{11\to10}$. [x] Used as a model: $\Delta_{11\to9}$ = −0.6 for *RR*/*SS* and $\Delta_{11\to9}$ = +6.9 for *RS*/*SR*. [y] Used as a model: $\Delta_{11\to10}$ = −1.0 for *RR*/*SS* and $\Delta_{11\to10}$ = +0.9 for *RS*/*SR*. [z] Used as a reference. [aa] Used as a model: $\Delta_{11\to12}$ = 0 for *RR*/*SS* and $\Delta_{11\to12}$ = +1.0 for *RS*/*SR*. [ab] H_2O : MeOH (1 : 1) is used as a solvent. [ac] Used as a model: $\Delta_{11\to3}$ = +1.1 for *RR*/*SS* and $\Delta_{11\to3}$ = +0.2 for *RS*/*SR*. [ad] Water as a solvent. [ae] $E'_a = E_{a,11} + \Delta_{11\to3} + \Delta_{11\to12}$. [af] Protonation expected to decrease E_a by 13.5 kJ mol^{-1}, as highlighted by the protonation of **12** in a H_2O/MeOH mixture. See ref. 41. [ag] $E'_a = E_{a,11} + \Delta_{11\to9} + \Delta_{11\to12}$. [ah] Used as a model: $\Delta_{11\to9}$ = −1.8 for *RR*/*SS* and $\Delta_{11\to9}$ = +1.4 for *RS*/*SR*. [ai] Used as a model: $\Delta_{11\to12}$ = −2.0 for *RR*/*SS* and $\Delta_{11\to12}$ = −1.0 for *RS*/*SR*.

Table 5 Valence angles α <OHO$_P$> and <OHN>, and distances $d_{OH\cdots OP}$ and $d_{OH\cdots N}$ for conformers A,[a] B,[b] and C [c] of diastereoisomers of **4** and **6**

		α[d] (°)		Distances[d] (Å)		
Alkoxyamine	Conformer	<OHO$_P$>	<OHN>	$d_{OH\cdots OP}$	$d_{OH\cdots N}$	Δ_{IHB} [e]
RR/*SS*-**3**	**A**[a]	**148**	—[j]	**1.83**	—[e]	−0.7[f]
RS/*SR*-**3**	**A**[a]	**150**	—[j]	**1.83**	—[e]	−0.9[f]
RR/*SS*-**4**	**A**[a]	**148**	—[g]	**1.83**	6.55	−3.6[h]
	B[b]	—[g]	**149**	6.25	**2.06**	n.e.
	C[c]	—[g]	—[g]	6.79	6.87	n.e.
RS/*SR*-**4**	**A**[a]	**146**	—[g]	**1.85**	6.61	0[h]
	B[b]	—[g]	161	4.78	2.13	n.e.
	C[c]	—[g]	—[g]	6.68	8.05	n.e.
RR/*SS*-**6**	**A**[a]	170	—[g]	1.82	5.09	n.e.
	B[b]	—[g]	**136**	5.16	**2.11**	−0.7[i]
	C[c]	—[g]	—[g]	6.65	4.82	n.e.
RS/*SR*-**6**	**A**[a]	**173**	—[g]	**1.79**	4.56	+7.1[i]
	B[b]	—[g]	136	4.99	2.03	n.e.
	C[c]	—[g]	—[j,k]	4.91	4.84[k]	n.e.
RR/*SS*-**9**	**C**[c]	—[g]	—[j]	6.00	—[j]	n.e.
RS/*SR*-**9**	**A**[b]	**174**	—[j]	**1.79**	—[j]	+6.0[l]
RR/*SS*-**4**	X-ray	—[g]	—[g]	6.63	6.91	n.e.
RS/*SR*-**6**	X-ray	164	—[g]	1.96	4.29	n.e.

[a] Conformer exhibiting IHB between HO and P=O functions. [b] Conformer exhibiting IHB between OH and N functions. [c] The most stable conformer with no IHB. [d] Bold values denote the most stable conformers. [e] In kJ mol^{-1}. n.e. not eligible. [f] $\Delta_{IHB} = E_{a,3} - E_{a,8}$. [g] Not given because of too long $d_{H\cdots X}$ forbidding any IHB. See ref. 38. [h] $\Delta_{IHB} = E_{a,4} - E_{a,5}$. See the ESI. [i] $\Delta_{IHB} = E_{a,6} - E_{a,7}$. See the ESI. [j] Not available. [k] A medium strength IHB between the HO group and the N-atom of the nitroxyl moiety is observed: $d_{OH\cdots N}$ = 1.99 Å and <OHN> = 140°. [l] $\Delta_{IHB} = E_{a,9} - E_{a,10}$. See the ESI.

is, in general, strongly restricted in the nitroxide,[46,47] and likely in the alkoxyamine.

IHB in alkoxyamines

A quick glance at **3**, **4**, **6** and **9** shows that several types of IHBs may occur (Fig. 4). The occurrence of *interR* IHB for *RS*/*SR*-**9** has been reported in the literature.[29] It has been observed by X-ray,[29] NMR,[29] and IR[29] and is supported by DFT calculations and does not deserve more comments, as *RS*/*SR*-**9** is used as a model. Diastereoisomer *RR*/*SS*-**9** does not exhibit IHB.[29] The occurrence of *intraN* IHB for **3** was recently studied by NMR¶¶ [27] and supported by DFT calculations in this work (see the ESI† and Table 5) and does not deserve more comments. X-ray data, NMR analysis, and DFT calculations support IHB of type *interR*, *intraR*, and *intraN* (Fig. 4, 8, 10 and 14) for *RS*/*SR*-**6**, *RR*/*SS*-**6**, and *RS*/*SR*-**4**, respectively (see the ESI†). In contrast with diastereoisomer *RS*/*SR*-**6**, no IHB is observed in diastereoisomer *RR*/*SS*-**4** by X-ray analysis, although ^{31}P NMR supports the occurrence of *intraN* IHB, ^{1}H NMR supports the occurrence of *interN* IHB. The appealing 3-center IHB displayed in Fig. 8 is disregarded by DFT calculations (too high energy conformer).‖‖ On the other hand, DFT calculations show a small difference in energy of 2.5 kJ mol^{-1} between the stable conformer **B** and conformer **A**, more stable than **C** by 16 kJ mol^{-1}, meaning that a fast equilibrium between **B** and **A** likely accounts for the simultaneous occurrence of *intraN* and *interN* IHBs observed by NMR. This fast equilibrium requires fast bond rotation around the C–N bond of the group carrying the hydroxy function. This fast rotation is nicely supported both by the temperature dependence of *RR*/*SS*-**4** (not shown) and the kinetics and NMR observations reported for **2** and **3** (*vide supra*). The small difference in energy of 8 kJ mol^{-1} between diastereoisomers of **4** agrees with the small difference of 1.6 kJ mol^{-1} in E_a.

Influence of IHB on k_d

Several linear multiparameter relationships developed over the last two decades to investigate various effects involved in the changes in k_d [25,36] cannot account for the effect of IHB. In parallel with these relationships, the group additivity approach[48] provides E_a values predicted with a good accuracy using a scale developed a decade ago.[49] To use the group additivity approach, alkoxyamine **11** was selected as a benchmark, as it displays the nitroxyl fragment with the lowest functionalization in that series and a secondary aromatic alkyl fragment. Thus, estimated activation energies E'_a were determined (Table 4 and ESI†). Taking into account the small difference in polarity between the alkyl fragment carrying a pyridyl (σ_I = 0.06)[50,51] or a phenyl (σ_I = 0.07)[52] moiety, no significant difference was reported,[41] and the presence of the hydroxyl group capable of *intraR* IHB does not provide more than a 2-fold increase in k_d, as highlighted by the couples **6**/**9** and **4**/**3**. To unveil the effect of IHB on k_d, the hydroxyl group was protected by silylation in **2** and **5**, by methylation in **8**, and by acylation in **7** and **10**, to suppress the occurrence of IHB (see the ESI†). Kinetic results

¶¶In ref. 29, no *intraN* IHB is observed in X-ray data.

‖‖Indeed, a 3-center IHB (Fig. 8) would require a conformation for the aromatic ring exhibiting a 1,3-*syn* allylic destabilizing interaction with H10, whereas such an interaction does not occur for conformers **A** and **B**.

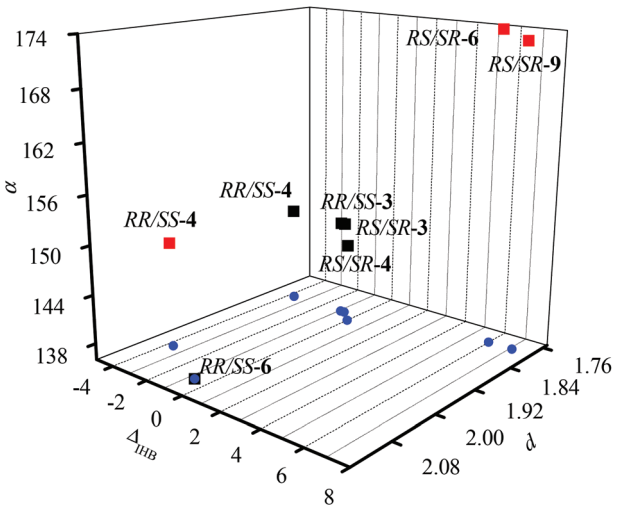

Fig. 15 A 3D plot highlighting the relationship between the energetic effect of IHB Δ_{IHB} (kJ mol^{-1}), IHB valence angle α (°), IHB distances $d_{OH\cdots X}$ (Å) for the diastereoisomers of 3, 4, 6 and 9. Black and red symbols are *intra* and *inter* fragment IHB, respectively (see Fig. 4). Blue dots are for projection on the *XY* plane.

showed that the 4 types of IHBs can be gathered into two main families: alkyl and nitroxyl fragments exhibiting *intra* IHB which show no significant differences (less than a factor 2) between the alkoxyamines carrying the free hydroxyl group (**3**, *RS*/*SR*-**4**, and *RR*/*SS*-**6**) and those carrying the protected hydroxyl group (**2**, *RS*/*SR*-**5**, and *RR*/*SS*-**7**) and *inter* IHB between alkyl and nitroxyl fragments which shows a clear 6–9-fold decrease in k_d between the alkoxyamines carrying the free hydroxyl group (diastereoisomers *RS*/*SR* of **6** and **9**) and those carrying the protected hydroxyl group (diastereoisomers *RS*/*SR* of **7** and **10**). Deeper insights into the geometrical parameters – the IHB valence angle α <OHX> and the IHB distance $d_{OH\cdots X}$ – ruling the strength of the IHB and its influence on k_d given by Δ_{IHB} (see Table 5) are unveiled by the 3D plot $f(\Delta_{IHB},d,\alpha)$ in Fig. 15. Indeed, *intra* IHB exhibits a very weak effect ($-1 < \Delta_{IHB} < 0$ kJ mol^{-1} except for *intraN* in *RR*/*SS*-**4**) associated with short H-bonds ($d_{OH\cdots X} < 1.9$ Å) and closed angles α ($\alpha < 150°$) denoting medium strength IHB,*** whereas *interR* IHB exhibits a strong effect ($\Delta_{IHB} > 6$ kJ mol^{-1}) associated with short H-bonds ($d_{OH\cdots X} \approx 1.8$ Å) and open angles α ($\alpha \approx 175°$) denoting strong IHB. As mentioned above, diastereoisomer *RR*/*SS*-**4** simultaneously displays *intraN* and *interN* IHBs and, thus, the decay of *RR*/*SS*-**4** is described in Scheme 5 with $K_1 = k_1/k_{-1}$ for the equilibrium constant between *interN* and *intraN* conformers, and k_2 and k_3 the rate constants for the homolysis of *interN* and *intraN* conformers, respectively. Taking into account that *interN* IHB makes a bond between nitroxyl and alkyl fragments as *interR* IHB does, the same effect is expected, *i.e.*, an increase in E_a in regard to the homologue with no IHB. Therefore, k_3

Scheme 5 Equilibrium between *interN* and *intraN* IHB and the subsequent homolysis.

must be smaller than k_2 which corresponds to *intraN* IHB noted to increase k_d (*vide supra*). Hence, disregarding k_3, and assuming both a fast equilibrium – supported by very close calculated energy levels (*vide supra*) – between conformers **B** (*interN*) and **A** (*intraN*) and the pre-equilibrium assumption ($k_{-1} \ggg k_2$ and $K_1 = k_1/k_{-1}$), k_d (considered as the apparent rate) is given as $k_d = k_1k_2/(k_{-1} + k_2)$ (eqn (2) or as $k_d = K_1k_2$ as in eqn (3), Scheme 5). As the decrease in E_a is in the expected range (see Table 4), the values of k_d should be very close to k_2, meaning that $K_1 \approx 1$ is in good agreement with the value estimated by DFT calculations, *i.e.*, $K_1 = 0.42$.†††

$$\frac{d[3^\bullet]}{dt} = \frac{k_1k_2}{k_{-1} + k_2}[interN] \quad (2)$$

$$\frac{d[3^\bullet]}{dt} = K_1k_2\cdot[interN] \quad (3)$$

Solvent effect on k_d

The solvent effect in alkoxyamines does not increase too much interest despite the very amazing results recently reported, such as a striking 1500-fold increase in k_d from *t*-BuPh to water as solvents or a slight but clear 5–20-fold increase in k_d for homologue alkoxyamines of **12**.[53,54] Solvent effects for **3**,[27] **9**,[29] and **12** [41] have been previously reported. Alkoxyamines **4**, **6**, **9** and **12** show a small *ca.* 1.5–3-fold increase in k_d, as expected from the literature,[53,54] except for *RS*/*SR*-**4**, *RS*/*SR*-**6** and *RS*/*SR*-**9**. The 3-fold and 5-fold increases in k_d for diastereoisomers *RS*/*SR* of **6** and **9** are ascribed to the suppression of IHB from *t*-BuPh to water/MeOH as solvents. The slight 4.5-fold increase in k_d observed for *RS*/*SR*-**4**, from *t*-BuPh to water/MeOH as solvents, might be ascribed to the suppression of stabilizing IHB which balances the steric strain due to the configuration. The unexpected slight *ca.* 2-fold decrease in k_d for **3** is ascribed to a better solvation of the alkoxyamine, and hence a better stabilization, and higher E_a from *t*-BuPh to water/MeOH as solvents than for the other alkoxyamines investigated.

For protonated alkoxyamines **4H+**, **6H+** and **12H+**, a 3–12-fold increase in k_d is observed and is ascribed to intimate ion pair dissociation and solvation effects,[55] except for *RS*/*SR*-**6**, for which a 25-fold increase in k_d is observed due to the combination of IHB suppression and intimate ion pair dissociation.

Effect of protonation on k_d

A *ca.* 10-fold and 60-fold increase in k_d for **12** in *t*-BuPh and water/MeOH as solvents was reported upon protonation. Amazingly, the protonation effect for **4**, *i.e.*, a *ca.* 6-fold and

*** The weak effect of IHB in *RR*/*SS*-**6** is due to a weak IHB (the weakest of those investigated), as highlighted by its longest $d_{OH\cdots X}$ and its closed angle α.

††† For such molecules, a difference of 2.5 kJ mol^{-1} in energy is in the limit of accuracy and reliability of the method.

12-fold increase in *t*-BuPh and water/MeOH as solvents, respectively, and that for **6**, *i.e.*, a 3-fold and *ca*. 8-fold increase (for the *RR*/*SS* diastereoisomer) in *t*-BuPh and water/MeOH as solvents, respectively, are less strong than that for **12**, although **6** and **4** exhibit structures very similar to that of **12**! Suppressing IHB in water/MeOH for *RS*/*SR*-**6H+** affords a 20-fold increase in k_d upon protonation. This surprising lower effect of protonation for **4** and **6** is ascribed to the better solvation of the alkoxyamine for **4** and **6** than that for **12**, due to the presence of the hydroxyl group affording the better stabilization of the starting alkoxyamine, which partly balances the polar effect due to protonation.

Experimental section

Alkoxyamines **3** were prepared as previously reported,[26] with the modification of the first step. All solvents and reactants for the preparation of alkoxyamines were used as received. Routine reaction monitoring was performed using silica gel 60 F_{254} TLC plates; spots were visualized upon exposure to UV light and a phosphomolybdic acid solution in EtOH as a stain revealed by heating. Purifications were performed on a Reveleris® X2 flash chromatography system (BUCHI, Switzerland); a solvent delivery system: high pressure HPLC pumps; pump flow rate: 1–200 mL min^{-1}; maximum pressure: 200 psi; gradients: linear (see Fig. 5SI† for the profile); UV wavelength range: 200–500 nm; flash Reveleris® and GraceResolv™ cartridges: silica 40 μm, silica weight (g): 4, 12, 24, 48, 80 and 120. ^{1}H, ^{13}C, and ^{31}P NMR spectra were recorded in $CDCl_3$ on a 300 or 400 MHz spectrometer. Chemical shifts (δ) in ppm were reported using residual non-deuterated solvents as the internal reference for ^{1}H and ^{13}C-NMR spectra, and as an internal capillary filled with 85% H_3PO_4 for ^{31}P-NMR spectra. High-resolution mass spectra (HRMS) were recorded on a SYNAPT G2 HDMS (Waters) spectrometer equipped with a pneumatically assisted atmospheric pressure ionization source (API). Positive mode electrospray ionization was used on samples: electrospray voltage (ISV): 2800 V; opening voltage (OR): 20 V; nebulizer gas pressure (nitrogen): 800 L h^{-1}. Low resolution mass spectra were recorded on an ion trap AB SCIEX 3200 QTRAP instrument equipped with an electrospray source. The parent ion $[M + H]^+$ is quoted.

Diethyl (1-((1-hydroxy-2-methylpropan-2-yl)amino)-2,2-dimethylpropyl)phosphonate (3b)

Under N_2, 2-methyl-2-aminopropanol **3a** (6.8 g, 1.1 eq., 76.7 mmol) was added dropwise to a solution of pivalaldehyde (6.0 g, 1 eq., 69.7 mmol) in pentane (50 mL). The solution was heated at 65 °C with a Dean–Stark device for 2 days. Then, pentane was evaporated and diethylphosphite (10.6 g, 1.1 eq., 76.7 mmol) was added at r.t., and the mixture was heated at 45 °C for seven days. The solution was acidified with 1 M HCl (50 mL), and washed with dichloromethane (2 × 30 ml). The aqueous layer was basified with $NaHCO_3$ and then extracted with dichloromethane (2 × 20 ml), the organic layer was dried ($MgSO_4$), and the solvent was evaporated to yield aminophosphonate **3b** (16.1 g, 78%).[26]

Diethyl (1-((1-((*tert*-butyldimethylsilyl)oxy)-2-methylpropan-2-yl)amino)-2,2-dimethylpropyl) phosphonate (2b)

The same procedure as that for **3b** was applied to **2a**. **2a** (3 g, 1.1 eq., 16.23 mmol), pivalaldehyde (1.27 g, 1 eq., 14.75 mmol), pentane (20 mL) and diethylphosphite (2.2 g, 1.1 eq., 16.23 mmol). After flash-chromatography (gradient petroleum ether (PE)/AcOEt: 0% to 100% of AcOEt), aminophosphonate **2b** was isolated (3.8 g, 64%, colourless oil). ^{1}H NMR (300 MHz, $CDCl_3$) δ: 4.09 (qd, J = 7.1, 1.3 Hz, 4H), 3.32 (s, 2H), 2.81 (d, J_{H-P} = 17.0 Hz, 1H), 1.68 (s, 1H), 1.30 (t, J = 7.1 Hz, 6H), 1.06 (s, 3H), 1.04 (s, 9H), 0.99 (s, 3H), 0.90 (s, 9H), 0.03 (s, 6H). ^{13}C NMR (75 MHz, $CDCl_3$) δ: 72.8 (d, J_{C-P} = 1.8 Hz), 61.4 (d, J_{C-P} = 7.4 Hz), 61.0 (d, J_{C-P} = 7.6 Hz), 58.9 (d, J_{C-P} = 138.7 Hz), 54.2 (d, J_{C-P} = 1.6 Hz), 35.2, 35.1, 27.9 (d, J_{C-P} = 6.2 Hz, 2C), 25.9 (3C), 25.1 (d, J_{C-P} = 1.5 Hz), 24.2, 18.2, 16.5 (d, J_{C-P} = 4.6 Hz), 16.4 (d, J_{C-P} = 5.0 Hz), −5.5 (2C). ^{31}P NMR (162 MHz, $CDCl_3$) δ: 30.09. HRMS m/z (ESI) calcd for $C_{19}H_{45}NO_4PSi$ $[M + H]^+$ 410.2850, found: 410.2852.

(1-(Diethoxyphosphoryl)-2,2-dimethylpropyl)-(2-((*tert*-butyldimethylsilyl)oxy)-1,1-dimethylethyl)amino-*N*-oxyl radical (2$^\bullet$)

Aminophosphonate **2b** (1.0 g, 1 eq., 2.4 mmol) was dissolved in a mixture of EtOH/H_2O (3 : 1) (15 mL) and Na_2CO_3 (1.55 g, 6 eq., 14.6 mmol). Then, Oxone® (3.0 g, 4 eq., 9.8 mmol) was added in small portions at r.t. within 2 h under vigorous stirring. After completion, Et_2O (10 ml) was added, and the precipitate was filtered off. Et_2O was removed under vacuum. The aqueous phase was extracted with dichloromethane (2 × 15 ml), and dried over $MgSO_4$ and the solvents were evaporated under reduced pressure. The crude was purified by flash chromatography (gradient PE/AcOEt: 0% to 100% of AcOEt) and nitroxide **2$^\bullet$** was isolated (529 mg, 51%). HRMS m/z (ESI) calcd for $C_{19}H_{44}NO_5PSi\cdot$ $[M + H]^+$ 425.2721, found: 425.2720.

Diethyl (1-((1-((*tert*-butyldimethylsilyl)oxy)-2-methylpropan-2-yl)(1-phenylethoxy)amino)-2,2-dimethylpropyl) phosphonate (2)

To a suspension of CuBr (55 mg, 0.55 eq., 0.388 mmol) and Cu powder (49 mg, 1.1 eq., 0.78 mmol) in degassed benzene (argon bubbling for one hour) (3 mL) was added *N*,*N*,*N*′,*N*′,*N*″-pentamethyldiethylenetriamine (80 μL, 0.55 eq., 0.39 mmol). After stirring for 10 min, a solution of nitroxide **2$^\bullet$** (300 mg, 1 eq., 0.71 mmol) and (1-bromoethyl)benzene (103 μL, 1.1 eq., 0.78 mmol) in degassed benzene (3 mL) was transferred to the first solution. The mixture was allowed to stir for 12 h. The solution was diluted with Et_2O, quenched with a NH_4Cl sat. solution, washed with water and brine, and dried over $MgSO_4$. The solvents were evaporated under reduced pressure to give the crude product as a 1 : 1 mixture of diastereoisomers (^{31}P-NMR ratio). The crude product was purified by automatic

flash-chromatography (gradient PE/AcOEt: 0% to 100% of AcOEt) to yield alkoxyamines *RR*/*SS*-**2** (pale yellow oil, 119 mg, 32%) and *RS*/*SR*-**2** (pale yellow oil 123 mg, 33%). *RS*/*SR*-**2** ^{1}H NMR (300 MHz, $CDCl_3$) δ: 7.37 (d, J = 7.3 Hz, 2H), 7.17 (m, 3H), 5.18 (q, J = 6.4 Hz, 1H), 3.86 (m, 2H), 3.69 (d, J_{H-P} = 26.6 Hz, 1H), 3.58 (s, 2H), 3.38 (m, 1H), 3.21 (m, 1H), 1.48 (d, J = 6.5 Hz, 3H), 1.15 (m, 18H), 0.86 (m, 12H), 0.00 (s, 6H). ^{13}C NMR (75 MHz, $CDCl_3$) δ: 143.2, 127.9 (2C), 127.7 (2C), 127.3, 78.5, 70.0 (d, J_{C-P} = 139.2 Hz), 69.0, 65.1, 61.6 (d, J_{C-P} = 6.4 Hz), 58.5 (d, J_{C-P} = 7.5 Hz), 35.4 (d, J_{C-P} = 5.3 Hz), 30.5 (d, J_{C-P} = 6.0 Hz, 2C), 25.9 (3C), 23.4, 22.6, 21.2, 18.2, 16.3 (d, J_{C-P} = 5.6 Hz), 16.1 (d, J_{C-P} = 6.9 Hz), −5.4, −5.5. ^{1}P NMR (121 MHz, $CDCl_3$) δ: 24.98. *RR*/*SS*-**2** ^{1}H NMR (300 MHz, $CDCl_3$) δ: 7.45 (m, 5H), 5.13 (d, J = 6.8 Hz, 1H), 4.53 (m, 1H), 4.22 (m, 3H), 3.86 (d, J_{H-P} = 26.5 Hz, 1H), 3.24 (q, J = 9.9 Hz, 2H), 1.74 (d, J = 6.7 Hz, 3H), 1.49 (m, 6H), 1.40 (s, 9H), 1.06 (s, 3H), 1.03 (s, 3H), 0.98 (s, 9H), 0.00 (s, 6H). ^{13}C NMR (75 MHz, $CDCl_3$) δ: 145.5, 128.2 (2C), 127.1, 126.8 (2C), 85.4, 69.7 (d, J = 138.1 Hz), 69.6 (d, J = 1.6 Hz), 65.3, 61.6 (d, J = 6.3 Hz), 58.8 (d, J = 7.5 Hz), 35.7 (d, J = 6.1 Hz), 29.9 (d, J = 5.8 Hz, 2C), 25.8 (3C), 24.5, 23.7, 22.1, 18.0, 16.8 (d, J = 5.4 Hz), 16.2 (d, J = 6.7 Hz), −5.5, −5.6. ^{31}P NMR (121 MHz, $CDCl_3$) δ: 26.19. HRMS for *RR*/*SS*-**2** and *RS*/*SR*-**2** mixture m/z (ESI) calcd for $C_{27}H_{53}NO_5PSi$ $[M + H]^+$ 530.3425, found: 530.3425.

General procedure for TBS protection of alcohols 3a, 3b and 3 [32,56]

In a flask under N_2, alcohols **3a**, **3b** or **3** (1.0 eq.), *tert*-butyldimethylsilyl trifluoromethanesulfonate (1.5 eq.) and 2,6-lutidine (2 eq.) were stirred in dichloromethane at room temperature for 4 hours. A saturated $NaHCO_3$ solution was added and the layers were separated. The organic layer was dried over Na_2SO_4, filtered, and concentrated *in vacuo*. Purification was performed using flash chromatography, affording **2a**, **2b**, or **2** as an oil.

Hydrolysis [31] of silylated compound 2

In a flask under N_2, *RR*/*SS*-**2** or *RS*/*SR*-**2** (30 mg, 1 eq., 0.06 mmol) was dissolved in THF (2 mL), and tetra-*n*-butylammonium fluoride (1 M in THF) was added (68 μL, 1.2 eq., 0.07 mmol). After stirring for 1 hour at room temperature, THF was evaporated under reduced pressure and the crude was purified by automatic flash-chromatography (gradient PE/AcOEt: 0% to 100% of AcOEt) to yield alkoxyamine *RR*/*SS*-**3′** or *RS*/*SR*-**3′** with a yield higher than 90%.

Diethyl-(1-((1-hydroxy-2-methylpropan-2-yl)(1-(pyridin-2-yl) ethoxy)amino)-2,2-dimethylpropyl) phosphonate (4)

In an open flask, $MnCl_2$ (70 mg, 0.05 eq., 0.35 mmol) was added to a stirred solution of salen ligand (130 mg, 0.05 eq., 0.35 mmol) in i-PrOH. After 30 minutes of stirring at room temperature, a solution of **3**$^{\bullet}$ (2.2 g, 1 eq., 7.1 mmol) and 2-vinylpyridine (1.15 mL, 1.5 eq., 10.6 mmol) in i-PrOH was added first, and then solid $NaBH_4$ (1.07 g, 4 eq., 28.4 mmol) was added in small portions. The resulting suspension was stirred at room temperature for 4 h. It was then diluted with EtOAc and 1 M aq. HCl was carefully added. Solid $NaHCO_3$ was then added until neutralization. The layers were separated, and the organic phase was washed with water and brine, and dried over Na_2SO_4. The solvent was evaporated to give the crude product as a 1 : 2 mixture of diastereoisomers (^{31}P-NMR ratio). The diastereomers were separated by automatic flash column chromatography (gradient PE/AcOEt: 0% to 100% of AcOEt) to afford *RR*/*SS*-**4** (pale yellow crystal 560 mg, 19%) and *RS*/*SR*-**4** (pale yellow oil 1.01 g 35%). *RS*/*SR*-**4** ^{1}H NMR (300 MHz, $CDCl_3$) δ: 8.44 (dd, J = 5.1, 1.7 Hz, 1H), 7.59 (td, J = 7.7, 1.8 Hz, 1H), 7.45 (d, J = 7.8 Hz, 1H), 7.07 (ddd, J = 7.6, 4.8, 1.2 Hz, 1H), 5.20 (q, J = 6.5 Hz, 1H), 3.89 (d, J = 12.7 Hz, 1H), 3.67 (m, 4H), 3.57 (d, J_{H-P} = 26.5 Hz, 1H), 3.44 (d, J = 12.6 Hz, 1H), 1.57 (d, J = 6.6 Hz, 3H), 1.12 (s, 3H), 1.10 (s, 9H), 1.09 (s, 3H), 1.04 (t, J = 7.1 Hz, 3H), 0.98 (t, J = 7.1 Hz, 3H). ^{13}C NMR (75 MHz, $CDCl_3$) δ: 162.1, 148.6, 136.9, 122.3, 121.6, 78.7, 70.5 (d, J_{C-P} = 136.3 Hz), 70.0, 64.9, 61.7 (d, J_{C-P} = 6.6 Hz), 60.1 (d, J_{C-P} = 7.9 Hz), 35.3 (d, J_{C-P} = 4.0 Hz), 30.6 (d, J_{C-P} = 5.7 Hz, 3C), 26.9, 22.0, 20.4, 16.4 (d, J_{C-P} = 5.7 Hz), 15.9 (d, J_{C-P} = 6.8 Hz). ^{31}P NMR (121 MHz, $CDCl_3$) δ: 26.13. HRMS m/z (ESI) calcd for $C_{20}H_{38}N_2O_5P$ $[M + H]^+$ 417.2513, found: 417.2513. *RR*/*SS*-**4** ^{1}H NMR (400 MHz, $CDCl_3$) δ: 8.49 (m, 1H), 7.66 (td, J = 7.7, 1.8 Hz, 1H), 7.43 (d, J = 7.9 Hz, 1H), 7.15 (ddd, J = 7.6, 4.9, 1.2 Hz, 1H), 5.09 (q, J = 6.7 Hz, 1H), 4.64 (s, 1H), 4.17 (m, 4H), 3.62 (d, J_{H-P} = 26.4 Hz, 1H), 3.49 (d, J = 12.3 Hz, 1H), 3.04 (d, J = 12.4 Hz, 1H), 1.54 (d, J = 6.7 Hz, 3H), 1.33 (t, J = 7.1 Hz, 6H), 1.18 (s, 9H), 1.02 (s, 3H), 0.68 (s, 3H). ^{13}C NMR (101 MHz, $CDCl_3$) δ: 164.2, 148.7, 136.7, 122.4, 121.7, 86.3, 69.6 (d, J_{C-P} = 136.1 Hz), 67.5, 65.1, 62.0 (d, J_{C-P} = 6.6 Hz), 60.6 (d, J_{C-P} = 7.8 Hz), 35.8 (d, J_{C-P} = 4.6 Hz), 30.1 (d, J_{C-P} = 5.7 Hz, 3C), 26.8, 23.6, 23.2, 16.6 (d, J_{C-P} = 5.7 Hz), 16.4 (d, J_{C-P} = 6.6 Hz). ^{31}P NMR (162 MHz, $CDCl_3$) δ: 27.29. HRMS m/z (ESI) calcd for $C_{20}H_{38}N_2O_5P$ $[M + H]^+$ 417.2513, found: 417.2515.

Diethyl ((*R*)-1-((1-hydroxy-2-methylpropan-2-yl)((*S*)-1-(pyridin-2-yl)ethoxy)amino)-2,2-dimethylpropyl)phosphonate (*RS*/*SR*-5)

Alkoxyamine *RS*/*SR*-**4** (400 mg, 1 eq., 0.96 mmol) was dissolved in 20 mL THF, and pyridine was added (388 μL, 5 eq., 4.80 mmol). Silver nitrate (244 mg, 1.5 eq., 1.44 mmol) was added and after stirring for 5 minutes, *t*-butyldimethylsilyl chloride (217 mg, 1.5 eq., 1.44 mmol) was added and stirring was continued at room temperature overnight. At the end of the reaction period, the solution was washed with 10% $NaHCO_3$ solution and extracted with DCM. The combined organic phases were dried with $MgSO_4$ and the solvent was evaporated. The crude product was purified by flash chromatography (petroleum ether/AcOEt 7 : 3) to afford *RS*/*SR*-**5** (pale yellow oil, 341 mg, 67%).^{1}H NMR (400 MHz, $CDCl_3$) δ: 8.52 (ddd, J = 4.9, 1.8, 0.9 Hz, 1H), 7.60 (m, 2H), 7.11 (ddd, J = 7.3, 4.8, 1.5 Hz, 1H), 5.26 (q, J = 6.6 Hz, 1H), 3.87 (m, 2H), 3.77 (d, J_{H-P} = 26.7 Hz, 1H), 3.71 (m, 1H), 3.63 (s, 2H), 3.57 (m, 1H), 1.58 (d, J = 6.6 Hz, 3H), 1.17 (m, 18H), 1.03 (t, J = 7.1 Hz, 3H), 0.91 (s, 9H), 0.04 (2s, 6H). ^{13}C NMR (101 MHz, $CDCl_3$) δ: 162.5, 148.6, 136.1, 122.5, 122.1, 79.9, 69.8 (d, J_{C-P} = 137.0 Hz), 69.2, 65.4, 61.3 (d, J_{C-P} = 6.4 Hz), 59.1 (d, J_{C-P} = 7.6 Hz), 35.5 (d, J_{C-P} = 5.1 Hz), 30.3 (d, J_{C-P} = 5.9 Hz), 25.9 (5C), 23.2, 22.8, 20.2,

18.3, 16.4 (d, J_{C-P} = 5.8 Hz), 16.1 (d, J_{C-P} = 7.0 Hz), −5.4 (2C). ^{31}P NMR (162 MHz, $CDCl_3$) δ: 25.22. HRMS *m*/*z* (ESI) calcd for $C_{26}H_{52}N_2O_5PSi$ $[M + H]^+$ 531.3378, found: 531.3380.

Diethyl((*R*)-1-((1-hydroxy-2-methylpropan-2-yl)((*R*)-1-(pyridin-2-yl)ethoxy)amino)-2,2-dimethylpropyl)phosphonate (*RR*/*SS*-5)

The same procedure as that for *RS*/*SR*-**5** was applied to *RR*/*SS*-**4**. *RR*/*SS*-**4** (210 mg, 1 eq., 0.5 mmol), 10 mL THF, pyridine (203 μL, 5 eq., 2.52 mmol), silver nitrate (128 mg, 1.5 eq., 0.76 mmol), *t*-butyldimethylsilyl chloride (114 mg, 1.5 eq., 0.76 mmol). *RR*/*SS*-**5** (pale yellow oil, 157 mg, 59%). ^{1}H NMR (400 MHz, $CDCl_3$) δ: 8.53 (ddd, *J* = 4.9, 1.8, 0.9 Hz, 1H), 7.66 (td, *J* = 7.7, 1.8 Hz, 1H), 7.34 (d, *J* = 7.8 Hz, 1H), 7.15 (ddd, *J* = 7.5, 4.9, 1.2 Hz, 1H), 5.13 (q, *J* = 6.8 Hz, 1H), 4.37 (m, 1H), 4.09 (m, 3H), 3.73 (d, J_{H-P} = 26.2 Hz, 1H), 3.12 (s, 2H), 1.59 (d, *J* = 6.8 Hz, 3H), 1.36 (t, *J* = 7.1 Hz, 3H), 1.30 (t, *J* = 7.1 Hz, 3H), 1.23 (s, 9H), 0.88 (s, 3H), 0.83 (s, 3H), 0.81 (s, 9H), −0.14 (2s, 6H). ^{13}C NMR (75 MHz, $CDCl_3$) δ: 164.5, 148.8, 136.2, 122.1, 121.7, 86.4, 69.8 (d, J_{C-P} = 138.3 Hz), 69.3 (d, J_{C-P} = 1.4 Hz), 65.4, 61.6 (d, J_{C-P} = 6.4 Hz), 58.9 (d, J_{C-P} = 7.5 Hz), 35.8 (d, J_{C-P} = 6.0 Hz), 29.8 (d, J_{C-P} = 5.8 Hz), 25.8 (3C), 23.3, 23.0, 22.6, 18.1, 16.8 (d, J_{C-P} = 5.5 Hz), 16.2 (d, J_{C-P} = 6.8 Hz), −5.6 (2C). ^{31}P NMR (162 MHz, $CDCl_3$) δ: 26.11. HRMS *m*/*z* (ESI) calcd for $C_{26}H_{52}N_2O_5PSi$ $[M + H]^+$ 531.3378, found: 531.3380.

2-Bromo-2-(pyridin-2-yl)ethyl acetate (6b)

2-(Pyridin-2-yl)ethyl acetate **6a** (2.0 g, 1 eq., 12.0 mmol), *N*-bromosuccinimide (2.4 g, 1.1 eq., 13.2 mmol) and benzoyl peroxide (0.03 g, 0.01 eq., 0.12 mmol) were mixed with CCl_4 (100 mL). An argon bubbled solution was refluxed (77 °C). The reaction was monitored by thin layer chromatography (TLC) after until complete disappearance of **6a**. The solution was then quenched and washed with $NaHCO_3$ sat., and the aqueous phases were extracted with CH_2Cl_2. The combined organic layers were washed with water, dried over $MgSO_4$ and concentrated under reduced pressure. The crude product was subjected to automatic flash-chromatography (gradient PE/AcOEt: 0% to 100% of AcOEt) to yield bromide **6b** (2.02 g, 69%). ^{1}H NMR (400 MHz, $CDCl_3$) δ: 8.59 (d, *J* = 5.6 Hz, 1H), 7.70 (t, *J* = 8.6 Hz, 1H), 7.42 (d, *J* = 7.9 Hz, 1H), 7.28–7.20 (m, 1H), 5.18 (t, *J* = 7.1 Hz, 1H), 4.73 (d, *J* = 7.1 Hz, 2H), 2.02 (s, 3H). ^{13}C NMR (101 MHz, $CDCl_3$) δ: 170.3, 156.7, 149.4, 137.3, 123.6, 123.1, 66.3, 49.1, 20.7. HRMS (ESI) calc. for $C_9H_{11}NO_2Br$ $[M + H]^+$: 243.9968; found: 243.9967.

Diethyl-(1-(*tert*-butyl-(2-hydroxy-1-(pyridin-2-yl)ethoxy)amino)-2,2-dimethylpropyl) phosphonate (6)

To a suspension of CuBr (660 mg, 0.55 eq., 4.6 mmol) and Cu powder (580 mg, 1.1 eq., 9.1 mmol) in degassed benzene (argon bubbling for one hour) (30 mL) was added *N*,*N*,*N*′,*N*′,*N*″-pentamethyldiethylenetriamine (1 mL, 0.55 eq., 4.6 mmol). After stirring for 10 min, a solution of **6**$^\bullet$ (2.68 g, 1.1 eq., 9.1 mmol) and bromide **6b** (2.0 g, 1 eq., 8.3 mmol) in degassed benzene (30 mL) was cannulated into the first solution. The mixture was allowed to stir for 12 h. The solution was diluted with EtOAc, quenched and washed with 50% (v/v) aq. ammonia solution and $NaHCO_3$ saturated solution, and dried over $MgSO_4$. The solvents were evaporated under reduced pressure. The crude product (1.1 g, 1 eq., 2.4 mmol) with a 1 : 4 diastereomeric ratio (^{31}P NMR ratio) was dissolved in MeOH (7 mL), and a solution of K_2CO_3 (663 mg, 2 eq., 4.8 mmol) in H_2O (7 mL) was added at once to the flask. The solution was allowed to stir for 3 days and then quenched with water. The aqueous phase was extracted with CH_2Cl_2 and dried over $MgSO_4$, and the solvents were evaporated under reduced pressure. The crude product was subjected to automatic flash-column chromatography (PE/acetone 7 : 3) to afford *RS*/*SR*-**6** (144 mg) and *RR*/*SS*-**6** (490 mg) as colourless oils, corresponding to a total yield of 634 mg (63%). *RS*/*SR*-**6** ^{1}H NMR (400 MHz, $CDCl_3$) δ: 8.53 (d, *J* = 4.8 Hz, 1H), 7.64 (t, *J* = 7.7 Hz, 1H), 7.37 (d, *J* = 7.7 Hz, 1H), 7.18–7.09 (m, 1H), 5.93 (t, *J* = 6.9 Hz, 1H), 5.11 (s, 1H), 4.44 (dd, *J* = 16.5, 7.7 Hz, 1H), 4.28 (dd, *J* = 16.7, 9.4 Hz, 1H), 4.21–4.09 (m, 2H), 4.02 (dd, *J* = 15.8, 7.9 Hz, 1H), 3.84 (dd, *J* = 15.1, 8.5 Hz, 1H), 3.43 (d, J_{H-P} = 27.6 Hz, 1H), 1.38 (t, *J* = 7.8 Hz, 3H), 1.34 (t, *J* = 7.6 Hz, 3H), 1.25 (s, 9H), 0.92 (s, 9H). ^{13}C NMR (101 MHz, $CDCl_3$) δ: 160.8, 149.0, 136.0, 122.7, 122.3, 91.0, 68.8 (d, J_{C-P} = 139.6 Hz), 65.0, 62.1, 62.1, 59.8 (d, *J* = 7.6 Hz), 35.8 (d, *J* = 5.1 Hz), 30.9 (d, *J* = 5.8 Hz, 2C), 28.1 (3C), 16.7 (d, *J* = 5.5 Hz), 16.24 (d, *J* = 7.0 Hz). ^{31}P NMR (162 MHz, $CDCl_3$) δ: 27.16. HRMS (ESI) calc for $C_{20}H_{38}N_2O_5P^+$: 417.2513 $[M + H]^+$; found: 417.2512. *RR*/*SS*-**6** ^{1}H NMR (400 MHz, $CDCl_3$) δ: 8.48 (d, *J* = 5.5 Hz, 1H), 7.73 (s, 1H), 7.65 (t, *J* = 8.5 Hz, 1H), 7.20–7.13 (m, 1H), 5.29 (t, *J* = 5.6 Hz, 1H), 4.72 (s, 1H), 4.34 (dd, *J* = 11.2, 5.3 Hz, 1H), 4.01 (dd, *J* = 11.2, 6.0 Hz, 1H), 3.96–3.83 (m, 2H), 3.73–3.60 (m, 2H), 3.46 (d, J_{H-P} = 26.7 Hz, 1H), 1.25 (s, 9H), 1.21 (s, 9H), 1.13 (t, *J* = 7.1 Hz, 3H), 1.03 (t, *J* = 7.1 Hz, 3H). ^{13}C NMR (101 MHz, $CDCl_3$) δ: 159.7, 148.2, 136.4, 123.3, 122.6, 80.5, 70.2 (d, J_{C-P} = 138.8 Hz), 64.7, 62.2, 61.3 (d, *J* = 6.7 Hz), 59.8 (d, *J* = 7.7 Hz), 35.4, 35.3, 30.8 (d, *J* = 5.9 Hz, 2C), 28.1 (3C), 16.3 (d, *J* = 6.0 Hz), 16.0 (d, *J* = 6.9 Hz). ^{31}P NMR (162 MHz, $CDCl_3$) δ: 24.48. HRMS (ESI) calc for $C_{20}H_{38}N_2O_5P^+$: 417.2513 $[M + H]^+$; found: 417.2511.

(*S*)-2-((*tert*-Butyl((*R*)-1-(diethoxyphosphoryl)-2,2-dimethylpropyl)amino)oxy)-2-(pyridin-2-yl)ethyl acetate (*RS*/*SR*-7)

RS/*SR*-**6** (144 mg, 1 eq., 0.35 mmol) was diluted in CH_2Cl_2 (5 mL) and triethylamine (0.2 mL, 4 eq., 1.4 mmol) was added. After 2 minutes, acetic anhydride (0.1 mL, 3 eq., 1.1 mmol) was added slowly *via* a syringe. The reaction was allowed to stir for 3 days and was then quenched with a saturated aqueous solution of $NaHCO_3$. The solution was extracted with CH_2Cl_2. The combined organic extracts were dried with $MgSO_4$, filtered, and concentrated under vacuum. The crude was purified by automatic flash-column chromatography (petroleum ether/acetone 9 : 1) to yield *RS*/*SR*-**7** (140 mg, 90%) as a white solid. ^{1}H NMR (300 MHz, $CDCl_3$) δ: 8.54 (d, *J* = 4.7 Hz, 1H), 7.66 (t, *J* = 7.7 Hz, 1H), 7.36 (d, *J* = 7.8 Hz, 1H), 7.21–7.12 (m, 1H), 5.30 (dd, *J* = 7.7, 4.2 Hz, 1H), 4.84 (dd, *J* = 10.9, 4.2 Hz, 1H), 4.69–4.59 (m, 1H), 4.48–4.33 (m, 1H), 4.21 (td, *J* = 16.6, 8.9 Hz, 1H), 4.03 (m, *J* = 17.2, 12.7, 7.2 Hz, 2H), 3.35 (d, J_{H-P} = 26.1 Hz,

1H), 1.79 (s, 3H), 1.36 (t, J = 6.4 Hz, 3H), 1.31 (t, J = 7.0 Hz, 3H), 1.23 (s, 9H), 0.87 (s, 9H). ^{13}C NMR (101 MHz, $CDCl_3$) δ: 170.1, 160.1, 148.8, 135.9, 123.3, 122.6, 87.5, 69.5 (d, J_{C-P} = 138.9 Hz), 65.7, 61.8 (2C), 61.7 (d, J = 6.4 Hz), 59.3 (d, J = 7.4 Hz), 35.8 (d, J = 5.4 Hz), 30.1 (d, J = 5.8 Hz, 2C), 28.4 (3C), 20.7, 16.8 (d, J = 5.4 Hz), 16.3 (d, J = 6.8 Hz). ^{31}P NMR (121 MHz, $CDCl_3$) δ: 25.27. HRMS (ESI) calc for $C_{22}H_{40}N_2O_6P^+$: 459.2619 $[M + H]^+$; found: 459.2624.

(*R*)-2-((*tert*-Butyl((*R*)-1-(diethoxyphosphoryl)-2,2-dimethylpropyl)amino)oxy)-2-(pyridin-2-yl)ethyl acetate (*RR*/*SS*-7)

The same procedure as that for *RS*/*SR*-7 was applied to *RR*/*SS*-**6**. *RR*/*SS*-**6** (490 mg, 1 eq., 1.18 mmol), CH_2Cl_2 (10 mL), triethylamine (0.5 mL, 4 eq., 3.5 mmol), acetic anhydride (0.3 mL, 3 eq., 3 mmol) flash-column chromatography (PE/acetone 9 : 1) *RR*/*SS*-7 (343 mg, 65%) as a colorless solid. ^{1}H NMR (300 MHz, $CDCl_3$) δ: 8.55 (d, J = 4.8 Hz, 1H), 7.69–7.57 (m, 2H), 7.20–7.08 (m, 1H), 5.35 (dd, J = 6.5, 3.6 Hz, 1H), 4.76 (m, 2H), 3.88 (p, J = 7.2 Hz, 2H), 3.74–3.50 (m, 2H), 3.44 (d, J_{H-P} = 27.1 Hz, 1H), 1.86 (s, 3H), 1.23 (s, 9H), 1.19 (t, J = 7.1 Hz, 3H), 1.15 (s, 9H), 1.00 (t, J = 7.1 Hz, 3H). ^{13}C NMR (101 MHz, $CDCl_3$) δ: 170.6, 158.1, 148.7, 135.8, 124.6, 122.7, 80.8, 69.6 (d, J_{C-P} = 138.6 Hz), 64.1, 62.0, 61.4 (d, J = 6.6 Hz), 59.5 (d, J = 7.7 Hz), 35.3 (d, J = 4.4 Hz), 30.7 (d, J = 5.9 Hz, 2C), 28.0 (3C), 20.7, 16.3 (d, J = 5.9 Hz), 16.1 (d, J = 6.8 Hz). ^{31}P NMR (162 MHz, $CDCl_3$) δ: 24.27. HRMS (ESI) calc for $C_{22}H_{40}N_2O_6P^+$: 459.2619 $[M + H]^+$; found: 459.2623.

Kinetic measurements

The values of the homolysis rate constant k_d were determined by monitoring either the concentration of nitroxide by EPR or the concentration of alkoxyamine by ^{31}P NMR. For EPR, a sample tube filled with a solution of 10^{-4} M of each diastereoisomer in *tert*-butylbenzene or in H_2O/MeOH (1 : 1) was set in the EPR cavity. EPR signals were recorded. The temperature was controlled by using a BVT2000 temperature controlling unit. Measurements of k_d by ^{31}P NMR required the use of TEMPO as an alkyl radical scavenger. The NMR tubes were filled with a stock solution of 0.02 M of alkoxyamine in *tert*-butylbenzene or in H_2O/MeOH with 2 equiv. of TEMPO. Buffer solutions were used for specific pH conditions instead of H_2O. k_d values were given by eqn (4). Activation energies E_a were estimated using eqn (5) and the average frequency factor A = 2.4×10^{14} s^{-1}. The values of k_d and E_a are listed in Table 4.

$$\ln \frac{[\text{alkoxyamine}]_t}{[\text{alkoxyamine}]_0} = -k_d t \quad (4)$$

$$k_d = A e^{-E_a/RT} \quad (5)$$

Conclusion

Different types of IHBs exhibiting very different effects are highlighted. These effects depend on the strength of the IHB, which in turn is straightforwardly related to its geometric parameters – $d_{OH\cdots X}$ the distance for IHB and the IHB valence angle α. That is, strong *interR* IHBs are expected for α larger than 160° and $d_{OH\cdots X}$ smaller than 1.8 Å affording an increase in E_a (Tables 4 and 5). As geometric parameters – $\alpha \approx 150°$ and $d_{OH\cdots X} \approx 2.1$ Å – underline a weak IHB, *interN* IHB does not exhibit the same effect as that of *interR* IHB. Indeed, this *interN* IHB is weak enough that it is in equilibrium with the *intraN* IHB which, in turn, favours slightly the C–ON bond homolysis, *i.e.*, decreasing E_a. Nevertheless, a strong *interN* IHB is expected to afford the same effect as that of a strong *interR* IHB. *IntraN* and *intraR* IHBs exhibit features of IHB of intermediate strength – $\alpha < 150°$ and $d_{OH\cdots X} > 1.8$ Å – affording a decrease in E_a. However, the effect of *intraR* and *intraN* depends a lot on the strength of these IHBs at TS, that is, on the stereoelectronic requirement for the C–ON bond homolysis and on the stabilization of the products, *i.e.*, partly due to the strength of IHB. Hence, stronger IHBs in products than in starting materials stabilize TS and decrease E_a. This assumption is supported by the stronger IHB in **3**$^\bullet$ (α = 178° and $d_{OH\cdots X}$ = 1.57 Å) than in **3** and **4** (Table 5).‡‡‡ [57]

As a rule of thumb, one may assume that IHB between alkyl and nitroxyl fragments (*interN* or *interR* IHB) affords an increase in E_a which might be pictured as the cleavage of two bonds – C–ON bond and IHB – and that IHB inside each fragment (*intraN* or *intraR* IHB) affords a slight decrease in E_a provided the stabilization due to IHB is larger for the released radicals than that for the starting material. Otherwise, an increase in E_a might be expected.

This work highlights the combination of several effects – IHB, solvents, intimate ion pairs, and protonation – to strikingly decrease the alkoxyamine half-life time $t_{1/2}$, as highlighted by $t_{1/2}$ = 123 days for **6** in *t*-BuPh as a solvent at 37 °C and by $t_{1/2}$ = 14 hours for **6H+** in water/MeOH as a solvent at 37 °C, that is, a 210-fold increase in k_d. These results nicely highlight the potential of such alkoxyamines as switches for applications in biology.[17]

Conflicts of interest

There are no conflicts of interest to declare.

Acknowledgements

SRAM, PB, VR and GA thank Aix-Marseille Université and CNRS for support. SRAM and ME are grateful to the Russian Science Foundation (grant 15-13-20020) for supporting this work and to the Multi-Access Chemical Service Center SB RAS for spectral and analytical measurements. SRAM, VR, GA and JPJ are grateful to ANR for funding this project (ANR-14-CE16-0023-01). PN thanks the Ministère de la Recherche du Gabon.

‡‡‡A similar effect on remote IHB has already been reported in ref. 57. The authors would like to thank the reviewer for pointing this issue at TS.

Notes and references

1 D. H. Solomon, E. Rizzardo and P. Cacioli, *Eur. Pat. Appl* 135280, 1985; D. H. Solomon, E. Rizzardo and P. Cacioli, *US Patent* 4581429, 1986; *Chem. Abstr.*, 1985, **102**, 221335q.
2 *Nitroxide Mediated Polymerization: From Fundamentals to Applications in Materials Sciences*, ed. D. Gigmes, RSC Polymer Chemistry Series 19, Royal Society of Chemistry, London, 2016; and 513 references cited therein.
3 A. Studer, *Chem. Soc. Rev.*, 2004, **33**, 267–273.
4 L. Tebben and A. Studer, *Angew. Chem., Int. Ed.*, 2011, **50**, 5034–5068.
5 A. Studer, *Angew. Chem., Int. Ed.*, 2000, **39**, 1108–1111.
6 J. Xu, E. J. E. Caro-Diaz, L. Trzoss and E. A. Theodorakis, *J. Am. Chem. Soc.*, 2012, **134**, 5072–5075.
7 C. Wetter, K. Jantos, K. Woithe and A. Studer, *Org. Lett.*, 2003, **5**, 2899–2902.
8 V. Sciannamea, R. Jérôme and C. Detrembleur, *Chem. Rev.*, 2008, **108**, 1104–1126.
9 E. H. H. Wong, M. H. Stenzel, T. Junkers and C. Barner-Kowollik, *Macromolecules*, 2010, **43**, 3785–3793.
10 Y. Guillaneuf, D.-L. Versace, D. Bertin, J. Lalevée, D. Gigmes and J. P. Fouassier, *Macromol. Rapid Commun.*, 2010, **31**, 1909–1913.
11 E. Yoshida, *Colloid Polym. Sci.*, 2010, **288**, 1639–1643.
12 G. Audran, E. G. Bagryanskaya, P. Brémond, M. V. Edeleva, S. R. A. Marque, D. A. Parkhomenko, O. Y. Rogozhnikova, V. M. Tormyshev, E. V. Tretyakov, D. V. Trukhin and S. I. Zhivetyeva, *Polym. Chem.*, 2016, **7**, 6490–6499.
13 G. Audran, E. G. Bagryanskaya, M. V. Edeleva, S. R. A. Marque, D. A. Parkhomenko, E. V. Tretyakov and S. I. Zhivetyeva, *J. Polym. Sci.: Part A: Polym. Chem.*, 2017, submitted.
14 M. Q. Zhang and M. Z. Rong, *Polym. Chem.*, 2013, **4**, 4878.
15 B. Schulte, M. Tsotsalas, M. Becker, A. Studer and L. De Cola, *Angew. Chem., Int. Ed.*, 2010, **49**, 6881–6884.
16 R. K. Roy, A. Meszynska, C. E. Laure, L. Charles, C. Verchin and J.-F. Lutz, *Nat. Commun.*, 2015, **6**, 1–8.
17 G. Audran, P. Brémond, J.-M. Franconi, S. R. A. Marque, P. Massot, P. Mellet, E. Parzy and E. Thiaudière, *Org. Biomol. Chem.*, 2014, **12**, 719–723.
18 D. Moncelet, P. Voisin, N. Koonjoo, V. Bouchaud, P. Massot, E. Parzy, G. Audran, J.-M. Franconi, E. Thiaudière, S. R. A. Marque, P. Brémond and P. Mellet, *Mol. Pharmaceutics*, 2014, **11**, 2412–2419.
19 N. A. Popova, G. M. Sysoeva, V. P. Nicolin, V. I. Kaledin, E. V. Tretyakov, M. V. Edeleva, S. M. Balakhnin, E. L. Louschnikova, G. Audran and S. Marque, *Bull. Exper. Biol. Med.*, 2017, **164**(7), 61–65.
20 P. Brémond, A. Koïta, S. R. A. Marque, V. Pesce, V. Roubaud and D. Siri, *Org. Lett.*, 2012, **14**(1), 358–361.
21 G. Audran, E. Bagryanskaya, I. Bagryanskaya, P. Brmond, M. Edeleva, S. R. A. Marque, D. Parkhomenko, E. Tretyakov and S. Zhivetyeva, *Inorg. Chem. Front.*, 2016, **3**, 1464–1472.
22 G. Audran, E. Bagryanskaya, I. Bagryanskaya, M. Edeleva, S. R. A. Marque, D. Parkhomenko, E. Tretyakov and S. Zhivetyeva, *ChemistrySelect*, 2017, **2**, 3584–3593.
23 P. Nkolo, G. Audran, P. Brémond, R. Bikanga, S. R. A. Marque and V. Roubaud, *Org. Biomol. Chem.*, 2017, **15**, 6167–6176.
24 K. Matyjaszewski, S. Gaynor, D. Greszta, D. Mardare and T. Shigemoto, *J. Phys. Org. Chem.*, 1995, **8**, 306–315.
25 S. Marque, H. Fischer, E. Baier and A. Studer, *J. Org. Chem.*, 2001, **66**, 1146–1156.
26 S. Acerbis, D. Bertin, B. Boutevin and D. Gigmes, *Helv. Chim. Acta*, 2006, **89**, 2119–2132.
27 G. Audran, P. Brémond, S. R. A. Marque and T. Yamasaki, *J. Org. Chem.*, 2016, **81**, 1981–1988.
28 E. G. Bagryanskaya, P. Brémond, T. Butscher, S. R. A. Marque, D. Parkhomenko, V. Roubaud, D. Siri and S. Viel, *Macromol. Chem. Phys.*, 2015, **216**(5), 475–488.
29 P. Brémond, T. Butscher, V. Roubaud, D. Siri and S. Viel, *J. Org. Chem.*, 2013, **78**, 10524–10529.
30 C. Reichardt and T. Welton, *Solvent and Solvent Effect in Organic Chemistry*, Wiley-VCH, Weinheim, 2011.
31 E. J. Corey and A. Venkateswarlu, *J. Am. Chem. Soc.*, 1972, **94**, 6190.
32 E. J. Corey, H. Cho, C. Rücker and D. H. Hua, *Tetrahedron Lett.*, 1981, **22**, 3455.
33 R. Braslau, N. Naik and H. Zipse, *J. Am. Chem. Soc.*, 2000, **122**, 8421–8434.
34 K. K. Ogilvie, G. H. Hakimelahi, Z. A. Proba and D. P. C. McGee, *Tetrahedron Lett.*, 1982, **23**((19), 1997–2000.
35 K. Matyjaszewski, B. E. Woodworth, X. Zhang, S. G. Gaynor and Z. Metzner, *Macromolecules*, 1998, **31**, 5955–5957.
36 E. G. Bagryanskaya and S. R. A. Marque, in *Kinetic Aspects of Nitroxide-Mediated Polymerization*, RSC Polymer Chemistry Series, n° = 19, Nitroxide Mediated Polymerization: From Fundamentals to Applications in Materials Sciences, ed. D. Gigmes, Royal Society of Chemistry, 2016, ch. 2, pp. 45–113.
37 R. S. Rowland and R. Taylor, *J. Phys. Chem.*, 1996, **100**, 7384–7391.
38 G. A. Jeffrey and W. Saenger, *Hydrogen Bonding in Biological Structures*, Springer, Berlin, Heidelberg, 1994.
39 A. Krężel and W. Bal, *J. Inorg. Biochem.*, 2004, **98**, 161–166.
40 R. J. L. Andon, J. D. Cox and E. F. G. Herington, *Trans. Faraday Soc.*, 1954, **50**, 918–910.
41 G. Audran, M. Bim Batsiandzy Ibanou, P. Brémond, S. R. A. Marque, V. Roubaud and D. Siri, *Org. Biomol. Chem.*, 2013, **11**, 7738–7750.
42 M. J. Frisch, G. W. Trucks, H. B. Schlegel, G. E. Scuseria, M. A. Robb, J. R. Cheeseman, G. Scalmani, V. Barone, B. Mennucci, G. A. Petersson, H. Nakatsuji, M. Caricato, X. Li, H. P. Hratchian, A. F. Izmaylov, J. Bloino, G. Zheng, J. L. Sonnenberg, M. Hada, M. Ehara, K. Toyota, R. Fukuda, J. Hasegawa, M. Ishida, T. Nakajima, Y. Honda, O. Kitao, H. Nakai, T. Vreven, J. A. Montgomery Jr., J. E. Peralta, F. Ogliaro, M. Bearpark, J. J. Heyd, E. Brothers, K. N. Kudin, V. N. Staroverov, R. Kobayashi, J. Normand, K. Raghavachari, A. Rendell, J. C. Burant, S. S. Iyengar,

J. Tomasi, M. Cossi, N. Rega, J. M. Millam, M. Klene, J. E. Knox, J. B. Cross, V. Bakken, C. Adamo, J. Jaramillo, R. Gomperts, R. E. Stratmann, O. Yazyev, A. J. Austin, R. Cammi, C. Pomelli, J. W. Ochterski, R. L. Martin, K. Morokuma, V. G. Zakrzewski, G. A. Voth, P. Salvador, J. J. Dannenberg, S. Dapprich, A. D. Daniels, Ö. Farkas, J. B. Foresman, J. V. Ortiz, J. Cioslowski and D. J. Fox, *Gaussian 09 (Revision A.02)*, Gaussian, Inc., Wallingford, CT, 2009.

43 S. Marque, *J. Org. Chem.*, 2003, **68**, 7582–7590.

44 S. Acerbis, E. Beaudoin, D. Bertin, D. Gigmes, S. Marque and P. Tordo, *Macromol. Chem. Phys.*, 2004, **205**, 973–978.

45 A. Studer, K. Harms, C. Knoop, C. Müller and T. Schulte, *Macromolecules*, 2004, **37**, 27–34.

46 G. Audran, R. Bikanga, P. Brémond, J.-P. Joly, S. R. A. Marque and P. Nkolo, *J. Org. Chem.*, 2017, **82**, 5702–5709.

47 P. Nkolo, G. Audran, P. Brémond, R. Bikanga, S. R. A. Marque and V. Roubaud, *Tetrahedron*, 2017, **73**, 3188–3201.

48 S. W. Benson, *Thermochemical Kinetics. Methods for the Estimation of Thermochemical Data and Rate Parameters*, John Wiley & Sons, Inc., New York, 1968.

49 E. Beaudoin, D. Bertin, D. Gigmes, S. R. A. Marque, D. Siri and P. Tordo, *Eur. J. Org. Chem.*, 2006, 1755–1768.

50 C. Hansch, A. Leo and R. W. Taft, *Chem. Rev.*, 1991, **91**, 165–195.

51 D. Bertin, D. Gigmes, S. R. A. Marque and P. Tordo, *Macromolecules*, 2005, **38**, 2638–2650.

52 M. Charton, *Prog. Phys. Org. Chem.*, 1981, **13**, 119–251.

53 G. Audran, P. Brémond, S. R. A. Marque and G. Obame, *Polym. Chem.*, 2012, **3**, 2901–2908.

54 G. Audran, P. Brémond, S. R. A. Marque and G. Obame, *J. Org. Chem.*, 2012, **77**(21), 9634–9640.

55 G. Audran, P. Brémond, S. R. A. Marque and G. Obame, *J. Org. Chem.*, 2013, **78**, 7754–7757.

56 T. J. Barker and E. R. Jarvo, *Angew. Chem., Int. Ed.*, 2011, **50**, 8325–8328.

57 M. C. Foti, R. Amorati, G. F. Pedulli, C. Daquino, D. A. Pratt and K. U. Ingold, *J. Org. Chem.*, 2010, **75**, 4434–4440.